An Osteological Study of the Individuals Buried in Grave 3 at Wadi Faynan 100, Jordan

by

Serena DiBiase

A thesis
presented to the University of Waterloo
in fulfillment of the
thesis requirement for the degree of
Master of Arts
in
Public Issues Anthropology

Waterloo, Ontario, Canada, 2021

Author's Declaration

I hereby declare that I am the sole author of this thesis. This is a true copy of the thesis, including any required final revisions, as accepted by my examiners.

I understand that my thesis may be made electronically available to the public.

Abstract

The main objective of this thesis is to address the paucity of research focussing on human remains at Jordanian archaeological sites by conducting an osteological analysis of Early Bronze Age individuals from a charnel house excavated at Wadi Faynan 100 (WF100) in Southern Jordan. This research provides the first preliminary analysis of the remains at WF100. Five graves were excavated in total during the 2019 field season, however, the remains analyzed and discussed here are from one large charnel house (Grave 3). Osteological analyses include estimation of the minimum number of individuals, sex estimates, age-at-death estimates, and observations of pathology. During excavation within these charnel houses, significant looting was noted, thus the impacts of looting are also taken into consideration when considering the human remains from Grave 3. The minimum number of individuals from the Grave 3 assemblage was estimated to be fourteen adults and eight subadults. While the fragmentary and commingled nature of this collection limits the ability to determine sex and age-at-death, the analyses for Grave 3 identified one female and two males. The age range for individuals within this assemblage is 22-40 years for adults and 6 months-14 years for subadults. The individuals of Grave 3 primarily demonstrated osteoarthritis in the vertebrae, bony growth shown on two of the phalanges and several phalanges had enlarged muscle attachments. This thesis provides preliminary insights into the lives of those interred in the Grave 3 charnel house at Wadi Faynan 100, and as such, provide a useful reference for burials to be excavated at the site, as well as laying the groundwork for comparisons between the populations of WF100 and other EB I burials in Jordan.

Acknowledgments

I am very grateful for my time spent as a student in the Department of Anthropology at the University of Waterloo. Although, the time spent physically at the university was cut short due to COVID-19, I am forever indebted to technology for keeping me connected with my advisor, department staff and my cohort.

I would firstly, like to give a big thank you to my supervisor Dr. Alexis Dolphin. I am grateful for the opportunity to study with her and for the constant feedback, support, and immense knowledge she has given me the past 19 months. Without her guidance and knowledge, this thesis would not have been possible. I would also like to thank Dr. Alexis Dolphin and Dr. Russell Adams for allowing me to study the remains recovered in 2019 from the Barqa Landscape Project and allowing me to take them home for analysis when the labs shut down on campus.

Thank you to my committee members, Dr. Alexis Dolphin, Dr. Russell Adams, and Dr. Maria Liston, for taking the time to review my thesis.

Thank you to the Department of Anthropology for making the transition into a graduate program smooth and providing support and guidance during my entire time here as a student. To my cohort, the little time we were able to spend together was very memorable and I am grateful for technology and being able to have zoom catchups every few weeks.

Thank you to my family and friends for the unwavering support over the past 19 months. To my parents, Graziano and Paola, thank you for consistently cheering me on from day one and allowing me to turn the basement into an at-home laboratory. To my boyfriend, Joseph Greco, thank you for your support, patience and reminders to take breaks every once and a while.

Finally, to the individuals buried at Wadi Faynan 100, who were the centre of my research, it was a privilege and an honour to study and learn about you and I am forever grateful of the opportunity. I hope, in the future, more of your lives and stories will be told through what you left behind.

Table of Contents

List of Tables

List of Figures

Chapter 1: Looting as a Public Issue

1.1 Public Issues

This thesis provides not only an osteological assessment of human remains from an Early Bronze Age site in Jordan, but also integrates diverse literature from anthropologists and archaeologists who have worked/are currently working on archaeological sites in Jordan. From traveling to different countries and doing research with local people, to studying the remains of their ancestors, anthropologists have always relied on engagement with the publics who make their research possible, and who consume the products of their research. This thesis presents an examination of human remains from Wadi Faynan 100 (2019 Barqa Landscape Project [BLP2019]) in order to provide a preliminary glimpse into life and death at this Early Bronze Age site located in Southern Jordan. Jordan, like many other countries, faces a heritage and conservation crises due to the looting of archaeological sites, like WF100. Understanding why and how looting occurs at a site like WF100 is of relevance not only to academic archaeologists, but also to the publics who are implicated in this practice, or face losses to their cultural heritage and economic development because of it.

1.2 Why Be Concerned About Looting?

Today, looting is still happening at archaeological sites around the world at an alarming rate (Fabiani, 2018). The objects taken from a site are often sold as 'art' on the antiquities market (Hsieh, 2018; Lundén 2012; Rodríguez *et al*., 2017). A large part of archaeological work is knowing the context of an artifact when it is found *in situ.* Once an artifact is removed from its context, it loses much of its value to archaeologists because there is no relationship between

those objects to their archaeological context and the information on the culture of the people whose artifact that belongs to is lost (Blythe *et al*., 2018). Archaeologists work to prevent looting given the potential for damage to the sites themselves, but also because of this concern with an irreversible loss of information when artifacts are removed from their contexts without documentation —it is an ethical concern (Hsieh, 2018, Barker 2018). Many pots recovered, such as ones from Safi, may include a mixture of an herbal-based drug from a past time period (Newnham, 1996). If those pots are then sold on the illicit trades market, that information is lost to archaeologists. It was determined that many of the graves at WF100 were looted based on the discovery of candy wrappers and other modern-day materials found within the graves. The destruction of the graves, and not knowing what was taken, can leave gaps of knowledge when trying to understand the site. Looting is generated by market demand and the countries most affected are those that are poor and war-torn (Lundén 2012, Barker, 2018).

1.3 How the Illicit Trades Works

Much of the buying and selling on the illicit trades markets goes undetected by authorities because of the difficulty in prosecuting someone caught with looted objects. In many cases of looting, owners of the objects (whether it is a museum, private collector, or a body of government) will have to file a civil law case against the accused (Ulph 2011). There are also many people involved in the process of dealing with these stolen goods, so prosecuting all participants is difficult. The parties included in the process of dealing are the people that actually do the stealing or looting, those that are accomplices, dealers who sell these looted goods for a profit and the purchasers which may not always know the objects have been stolen/looted (Ulph

2011). As a result of so many people being involved, it can be difficult to determine who to prosecute.

This is made more difficult by the fact that the illicit market is quite secretive, and participants usually do not ask questions about the details of how items have been acquired (Ulph 2011). If no questions are asked, it can be hard to determine what knowledge, for example, the dealer or purchaser had when in contact with these artifacts. Additionally, art and antiquities are moved between countries to make tracing and detection more difficult (Ulph 2011). The reasoning behind this is that it will be more difficult to know the objects' origins once they have been removed and shipped between countries. All of this makes any investigation of individual participants in illicit trades networks very expensive and complicated (Ulph 2011).

1.4 Understanding Looting of Archaeological Sites

1.4.1 Wars and Military Conflicts

Wars and military conflicts have had a significant impact when it comes to the looting of archaeological sites (Barker, 2018; Fabiani, 2018). The March 2011 civil unrest in Syria led to the damage of many cultural heritage sites. The damage was done intentionally and unintentionally by military action, ideologically motivated attacks, commercially inspired theft and looting, and unauthorized construction works (Brodie, 2015).

The destruction of sites and the loss of cultural heritage was also significant in the 2003 Iraq War, which may have been due to the invading states not being trained in how to safeguard heritage sites (Barker, 2018). Many countries such as the United States and the United Kingdom have ratified legislation to protect cultural heritage in times of conflict. The Hague Convention is one piece of legislation that requires state parties to adopt measures to safeguard cultural

property and refrain from using it in a manner that risks the site or object during conflict (Barker, 2018). The Hague Convention also establishes special military units to ensure respect for cultural property and cooperation with civilians (Barker, 2018).

Jordan has not been a major player – if at all – in regard to the wars surrounding the country. With the 1991 Gulf War, Jordan did fall into an economic recession, however, which encouraged people to loot sites and sell the artifacts for profit. In an article published in *The Guardian Weekend* (1996), Newnham says that, during the Gulf War, an average person at Safi would earn £8 a day growing their tomatoes but local dealers are offering them £1 per four pots, no matter what size (Newnham, 1996). As a result of that, the cemetery at Safi was looted every night. Simon Edge (1991) describes Jordan's economic crisis during the Gulf War as,

> "The government's initial calculation was that losses incurred as a result of the crisis would cost the country as much as 50 per cent of gross domestic product (GDP) in the first year. The losses are caused by the disappearance of aid and remittance income from Iraq and Kuwait, the severance of trade relations with Baghdad, and the collapse of transit trade through the port of Aqaba. Shipping traffic to Jordan itself has also been badly affected by a sharp increase in insurance rates and by what local shippers see as unjustified harassment by the US navy in the Red Sea" (Edge 1991, 1).

Communities with few economic opportunities may see an increase in looting because it may represent the least-bad choice, even if it provides a small amount of income (Barker, 2018). An economic crisis such as a recession can cause people to do whatever necessary to make money to support themselves and/or their families. In addition, the chaos brought about by military conflict and resulting economic hardships in the 1990s spawned the development of large illicit antiquities trading networks, such as that allegedly founded by Ghassan Rihani, an Amman resident, who was charged with overseeing illicit transport of archaeological materials from Iraq, Jordan and Syria to sell in London and other countries (Brodie, 2015).

1.4.2 Climate Change

Climate change can also have a significant impact on looting. One of the main climate change threats in the Middle Eastern context is water availability. Climate change can have effects on farmers in remote areas that survive solely on the crops they grow, but in more populated areas, less conflict is likely to occur given water re-allocation measures (Feitelson *et al*., 2012).

> "The framing of water issues and of climate change as security issues, and the subsequent subservience of water and environmental issues to the 'high politics' of the conflict may hinder the ability to undertake the adaptive measures that may mitigate the effects of climate change. Specifically looking at the water supply in Jordan, the authors note that the water resources available for the Palestinians under a 50% arbitrary allowance will not be enough to supply the peripheral agriculture" (Feitelson *et al.* 2012, 253).

Many peripheral farmers live within the Jordan Valley which in turn means they will be heavily affected by climate change and its impacts on water availability. Since Jordan is a country that relies heavily on agriculture, if there is less agricultural production in the Jordan Valley then it could have disastrous effects for the country, with those effects likely extending into the regions around as well (Feitelson *et al*. 2012). Many of the lands owned by the farmers are bordered by archaeological sites which can pose a problem to the farmers who may want to expand their land while adjusting to the pressures placed upon them by climate change.

1.4.3 Tourism

Jordan's economy relies heavily on tourism and frequently promotes its archaeological sites as popular tourist attractions. Many people will travel across the world to see archaeological sites such as Petra, Jerash and Nebo Mountain. Tourism in Jordan is the second largest private sector employer and the second highest producer of foreign exchange (Abu Al Haija, 2011). Many Jordanian citizens live and work nearby, or on, important historical and archaeological

sites. With the number of tourists growing every year, the Jordanian Government had to create new heritage policies over the last few decades. These policies include: (1) improving tourism infrastructure (airports, streets, hotels) in tourist zones; (2) rehabilitation of old centres, targeted mainly towards tourist needs; (3) increasing the involvement of the private sector in tourism projects; and (4) creating Special Economic Zones or Economic Development Zones in certain Jordanian areas, with a concentration in the development of tourist sectors (Abu Al Haija 2011).

This increased tourism to Jordan can also contribute to an increase in looting activity. As a result of the government creating new policies that specifically cater to tourism, some local communities within Jordan are suffering. People have been uprooted and moved to new locations in order to conserve the physical appearance of historic and ancient villages (such as Taybet Zaman, Kherbat Al Nawafleh, etc) (Abu Al Haija, 2011) to meet the growing needs of tourists. The traditional houses found in these villages, that have been there for centuries, are being modified and built into hotels, restaurants and gift shops (Abu Al Haija, 2011). Many people indigenous to these communities were aggravated with the government for capitalizing off their place of residence. Greater communication needs to be had between local communities and the Jordanian government.

There are several ways in which the Jordanian government can help find a balance between local communities and tourism and serve to prevent the circumstances that may lead to widespread looting of archaeological sites. One example from Abu Al Haija (2011) is, “The Jordanian regional and urban planning system should be reviewed in order to diversify the level of intervention according to the local particularities and needs” (99). Creating a stream of communication between the government and local communities can ease the tensions and help the government understand what they can do to help the communities and as a result, the

communities may also be able to help the government benefit from tourism. “The significance of space seen by locals is different from the Jordanian municipality’s or government technicians; for locals the spirit of place is conserved in its historical layers, including all kind of materials, forms and spiritual memory, which is in continuous evolution and transformation according to their specific needs” (Abu Al Haija 2011:99). The current debate on the ethics of looting is at a cross-roads, with one side being the living communities and their use of the material remains of the past to their own contemporary ends (Barker, 2018). Engaging local peoples in discussions about tourism and heritage can benefit all, and ideally lay the groundwork for sustainable development that does not see local people pushed to engage in looting activities.

1.5 Conclusion

The looting of archaeological sites is impacted by a complex set of inter-related activities and economic pressures. Selling looted objects on the illicit trades market is also something that is difficult to quantify. Data on looting and thefts in various countries around the Near East may be used to examine and/or identify objects originating from these regions as they appear on the antiquities market (Lundén, 2012). Looting may be carried out by organized networks of criminals who collect income from the objects they assemble from archaeological sites. But it can also be carried out by regular citizens who are expanding their farms in the face of climate change or facing economic hardship.

Looting today is still very prominent, not only in Jordan but in every place of the world too. Tracking the rate and volume of looting over time can help archaeologists and government officials work together to combat looting. Greater communication between Jordanian locals and the government officials can also prove beneficial. Jordan’s economy relies heavily on tourism

but, government and industry also cannot disregard the input of local stakeholders, especially those who are being relocated as a result of building new resorts and hotels. Understanding the reasons for looting can help in preventing the looting of archaeological sites, benefiting researchers and local peoples who value the wonderful cultural heritage of Jordan.

1.6 Venue for Publication

The intended venue for publication is the International Journal of Osteoarchaeology. This journal publishes papers that deal with all aspects of the study of human and animal bones from archaeological contexts (International Journal of Osteoarchaeology, n.d.). The main aim of this journal is to publish informed studies that analyze human and animal remains to provide detail and information about the behaviour and ideology of past cultures (International Journal of Osteoarchaeology, n.d.). As this thesis is an osteological study on the human remains found in the Wadi Faynan 100, it fits into the aims of this journal and helps to fill a gap in the literature about osteological human remains from Jordanian archaeological sites.

Chapter 2: The Individuals of Wadi Faynan 100

2.1 Introduction

2.1.1 Bioarchaeology in Jordan

Jordan is an area with incredible archaeological potential that has influenced the works of many scholars (Chesson, 1991, 2001; Lapp 1968, 1996; Rast & Shaub, 1979). One topic area that is generally under-represented in such works is an analysis of human remains found at sites scattered across Jordan, and the Middle East in general (Sheridan, 2017).

Many of the first explorers of Jordan (then Transjordan), beginning in 1805, were antiquarians and biblical scholars interested in historical or biblical sites (Adams, 2008). These early antiquarians were interested in sites with a focus on the "Holy Land" within Cisjordan and the Palestine (Adams, 2008). Once a British Mandate (1918-1946) was established in the region of Palestine and Transjordan, archaeologists found the region increasingly accessible, with those researchers laying the foundation for our current understanding of the archaeology and history of the region (Adams, 2008). Further propelled by the establishment of the Department of Antiquities, archaeology in Jordan has grown to support numerous field projects, publications, and heritage partnerships [for example, the restoration and rehabilitation project of Aqaba Castle (2016-2018)] (Department of Antiquities, 2019).

Wadi Faynan 100 is an Early Bronze Age (EBA) (3600 BC – 2200 BC) site (Adams, 2008; Adams *et al*., 2017; Barker *et al*., 2007; Philip, 2008), located in Southern Jordan. One key factor that aided in the development of Chalcolithic and Early Bronze Age societies at WF100 was the local elites trading metals with neighbouring villages (Barker *et al*., 2007). The Wadi Faynan region has significant evidence of metal working and it is one of the largest and most

well-preserved industrial landscapes of the ancient world (Adams *et al*. 2017; Adams and Genz 1995; Barker *et al*., 2007; Wright *et al*. 2013). Within the Wadi Faynan region, there is a long history of communities extracting and processing copper ores (Barker *et al*., 2007). Wadi Fidan 4 dates to the mid-fourth millennium BC (3600-3300BC) as the developmental phase of metallurgy (Adams *et al*., 2017). The large copper production centre of Khirbat Hamra Ifdan dates to the mid-third millennium BC (2600-2300 BC) (Adams 1999, 2000, 2002, 2006; Adams *et al*., 2017; Levy *et al*., 2002). All of these investigations have given researchers the ability to understand the evolution of early metallurgy spanning throughout the EBA, which was a change from small-scale, village level production (Adams 1999; Adams *et al*., 2017; Adams and Genz 1995), to very developed and large-scale production by the end of the period (Adams 1999; Adams *et al*., 2017; Levy *et al*., 2002).

There are numerous sites around Jordan where archaeological excavations have taken place. These sites include Bab adh-Dhra', Numeira, Tell el-Hammam, and Khirbat Faynan. Bab adh-Dhra is an Early Bronze Age site located approximately 150 kilometers to the north of WF100, near the Dead Sea, which appears to be a cemetery that people travelled to, with their dead, from the Kerak Plateau (Steele 1990). Bab adh-Dhra produced material from all periods of the Early Bronze Age, including the EB I, thus providing a good comparator for Wadi Faynan 100. EB 1A burials appeared as shaft and chamber graves about 1m in diameter, extended below ground (1-3m), and had several chambers radiating from the base of the shaft (Gregorika *et al.* 2019; Ortner & Frolich, 2007; Philip, 2008; Schaub and Rast, 1981). Tomb A 78 had a vertical circular shaft opening into four chambers, the entrance to each of which was closed by a stone (Ortner & Frolich, 2007; Philip, 2008; Schaub and Rast, 1981). Most of the burials at this site are secondary in nature, meaning that the remains were placed in these shaft burials after some prior

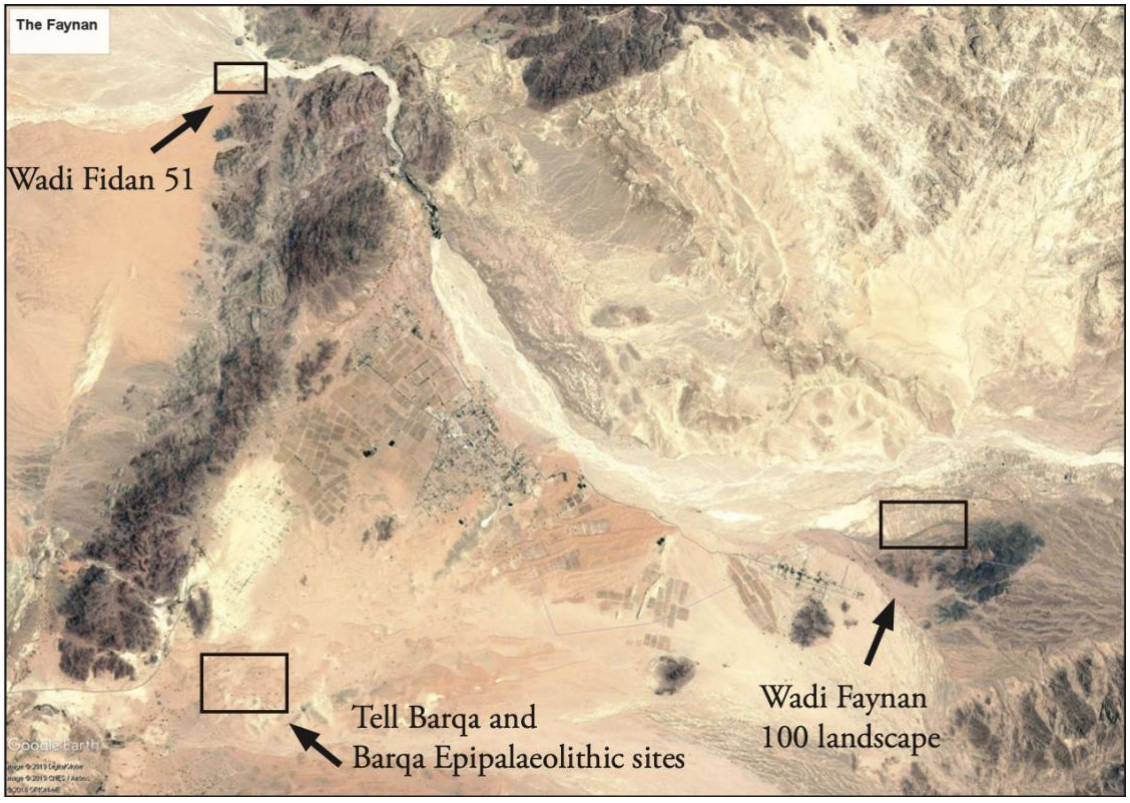

Figure 1: *Map of the Barqa Landscape Project 2019, research zones*

treatment of the body closer to the time of death (Chesson 2001; Lapp 1968; Polcaro *et al.* 2014; Rast & Schaub 1979). The skeletal remains were in a pile in the centre of each chamber with the skulls placed to the left of the pile, and grave goods (ceramic vessels) were placed around the edge of the chamber or to the right of the entrance (Philip, 2008). The graves contained adult (male and female) and child burials and seem to represent family groups (Chesson, 1999; Gregorika *et al.* 2019; Lapp, 1968; Ortner & Frolich, 2007, Philip, 2008).

EB II-III tombs were rectangular mud-brick structures called “charnel houses” and the skulls were often placed in a row to the left of the entrance and postcranial bones were piled in the centre (Lapp, 1968; Ortner & Frolich, 2007; Philip, 2008). The entrance was along the long side and had a stone threshold (Philip, 2008).

2.1.2 Wadi Faynan 100

Wadi Faynan 100 (WF100) is one of the few unploughed parts of the Faynan field system (Adams, 2020, personal communication). Wadi Faynan 100 was originally discovered in 1994

by the British Institute at Amman for Archaeology and History (BIAAH) reconnaissance survey and was found largely intact (Adams, 2020; Barker *et al*. 2007; Wright *et al.* 1998). It has since produced extensive Early Bronze Age artifacts (Wright *et al.* 1998; Barker *et al*. 2007). The region was originally owned by the Reshaydeh Bedouin tribe, but they showed no interest and rarely visited until they decided to re-populate the area because of the water resources available (Adams, 2020, personal communication). As the Reshaydeh settled into the new village they created and started practicing horticulture, it has resulted in the significant destruction of the built archaeology, with the exception of WF100 which has remained protected (Adams, 2020, personal communication).

The British Institute at Amman began recruiting academics to take an interest in the area and convinced Katherine Wright to begin a project at Faynan (Adams, 2020). Wright *et al.* conducted test excavations in 1996, with a limited budget and small team (Adams, 2020), and revealed that the site dates to the late fourth millennium or Early Bronze I (EBI) (3600-3300 BCE) (Wright *et al.* 1998). Surface collections were done in 1996 and 1997 by Wright and colleagues. In 1997, Wright *et al*. completed several operations during the field season. Operation 1 investigated Structure 10, finding hundreds of EB pottery sherds (Wright *et al*. 1998). Operation 2 began as a 5 x 12m north/south trench and later, it was extended and 70.50sq.m were exposed (Wright *et al*. 1998). Wall 1 ran along the terrace edge and continued across Operation 2 (Wright *et al*. 1998). Operation 1 and 2 were meant to investigate the overall size of WF100. Operation 3 was part of the south-eastern quadrant that covered an area of about 100 x 50m rising 5-10m above the rest of the site (Wright *et al*. 1998). The main goals of Operation 3 were to: 1) test the side of the site; 2) investigate the date of Wall 2; and 3) investigate Mound 4 and its relationship to Wall 2 and the character of deposits within it (Wright

et al. 1998). Operation 4 was laid out within a 15 x 15m area west of Operation 3.2 (Wright *et al*. 1998). Several phases of EB occupation were identified in deposits reaching a depth of 0.90m below the present surface (Wright *et al*. 1998). Very little was published on this project and not a lot was contextualized about what they observed (Adams, 2020, personal communication).

During the same time, Professor Barker, Professor Gilbertson and Professor Mattingly began the Faynan Landscape Survey (FLS) (Adams, 2020, personal communication; Barker *et al*., 2007). The FLS was a large-scale multi-disciplinary project that spent about seven years doing a detailed investigation of the natural environment, documenting all the surface archaeology (from prehistoric to Medieval), conducting a large scale surface collection of artefacts from the entire landscape, and developing a period by period synthesis of all the major periods of occupation (Pleistocene and Early Holocene; Chalcolithic and Earth Bronze Age, Iron Age, Romano-Byzantine, and Islamic and Modern period) (Adams, 2020, personal communication). All of the periods mentioned were documented in the surface distribution of the artifacts and built environment (Adams, 2020, personal communication).

WF100 remained relatively untouched by archaeologists until Dr. Russell Adams began his excavations in the area in 2013 and 2014. In 2013, work was done at Tell Barqa where a large fortification wall feature was discovered and subsequently, in 2014, the site of Wadi Fidan 51 was excavated with 4 trenches being opened to try dating and mapping the extent of the site (Adams *et al*., 2019). The work undertaken in 2019 aimed to complete several small projects in order to move the research done in 2013 and 2014 to publication (Adams *et al*., 2019). WF100 was excavated in the summer of 2019 as part of the Barqa Landscape Project 2019 (BLP)

Figure 2: *Wadi Faynan 100, Grave 3, Facing East*

directed by Dr. Russell Adams (*Figure 1*). The aim of this project was to do more research into ancient metal pollution by focusing on the Bronze Age (Adams *et al*. 2019). Another goal of the BLP was to excavate a sample of Early Bronze Age graves of human bones and teeth to better understand the impacts of copper production on the population (Adams *et al*. 2019).

When beginning the initial search for burials, significant looting was noted in several areas around the Faynan Basin. Areas that were harder to reach were searched for burials. A series of knolls near the southeastern end of the Wadi Faynan was designated as Faynan Cemetery 1 (Adams *et al*. 2019). In total, 5 graves were identified at WF100 itself. In this thesis, only Grave 3 from WF100 was focussed on because it provided the most osteological material. The human remains collected during the 2019 BLP excavations came from roughly rectilinear stone-built charnel houses (Adams *et al*. 2019). Graves 4 and 5 were also notable because they were surrounded by a double wall (Adams *et al*. 2019).

Grave 3 (*Figure 2*) was located on the east side of the WF100 downslope from Graves 1 and 2 (Adams *et al.* 2019). Grave 3 was chosen for excavation because the walls were well defined, and it was within close proximity to Graves 1 and 2 (Adams *et al.* 2019). Graves 1 and 2 showed significant signs of looting activity and with Grave 3 being on a hill but still within close proximity to the other Graves, the hope was that Grave 3 would have less of an impact of looting activity. The entrance of the grave was located within the north wall that was defined by two large stones on either side of the entrance wall (Adams *et al.* 2019). The length of the grave (north to south) was roughly 3m and the width (east to west) was 1.5m, and the depth was 1m (Adams *et al.* 2019).

Seven loci were found within Grave 3. Locus 1 was the disturbed layer that included backfill from looting and contained very fragmentary human and faunal bones (Adams *et al.* 2019). The fragmentary nature of the human bones could very well be as a result of the looting that was happening. Locus 2 was located near the south-eastern corner of the wall and contained articulated tarsals, metatarsals, and phalanges from an adult individual (Adams *et al.* 2019). Locus 3 was located along the southern wall of the grave and contained cranial and postcranial remains from a subadult (Adams *et al.* 2019), along with beads and an animal bone pendant. Locus 4 was located within the southern portion of the grave and contained human bone fragments and teeth from, potentially, one adult individual (Adams *et al.* 2019). Locus 5 and Locus 6 were in the northern portion of the grave with human bone and tooth fragments (Adams *et al.* 2019). Locus 99 was used to define the bottom portions of the grave (Adams *et al.* 2019). This Locus encompassed the catch-all of the remaining excavation of the grave, as well as the human remains found on the bedrock floor of the grave (Adams, 2020, personal communication).

2.1.3 Condition of the Remains at Wadi Faynan 100

This research intends to fill a gap in the archaeological record where there is a very limited body of research on human remains from Jordanian sites (Sheridan, 2017). Dr. Charlotte Roberts, in a chapter from *Early Prehistory of Wadi Faynan* (Finlayson and Mithen, 2007), discusses the difficulties of sex estimation using human remains from Wadi Faynan 16 (WF16) and argues that "without the ability to compare the remains with contemporary skeletal material from the same site and/or area of Jordan, it is unclear whether these, in fact, do represent female individuals at this site" (402). Roberts rightly points out the need for comparative data to be collected from archaeological human remains from Jordan in order to best complete her research with a degree of certainty.

There are several reasons for this gap in the archaeological record: 1) Near Eastern archaeological research can take a relatively long time in several regions; 2) the treatment of human remains has not always been adequate (e.g., the collapse of a storage shed at the WF Albright Institute of Archaeological Research in Jerusalem); and 3) there can also be legal issues when it comes to land claims in the southern Levant (Sheridan, 2017). This makes it particularly difficult to try and analyze human remains from the region with few works to compare/contrast to. This thesis analyzed the human remains found in Grave 3 at WF100 in order to help fill this gap in knowledge. One of the problems that Roberts faced, and that is commonly confronted by those excavating remains in Jordan, particularly from the EBA, is the commingled nature of the remains. In the past, researchers were not wanting to sort through commingled remains as they believed they were not worth analyzing (Sheridan, 2017). By incorporating the analysis of commingled remains into archaeological reports, or their own articles, researchers can ensure

that a wider variety of ancient lifeways are considered (Sheridan, 2017). This thesis can prove beneficial because of the commingled nature of the remains from WF100.

Despite the fragmentary and commingled nature of the osteological sample derived from the BLP 2019 excavations, recovery of remains was undertaken with exceptional care. This has been demonstrated through the successful reconstruction of 100+ teeth that were recovered from the assemblage (Tucciarone, 2020, personal communication).

2.2 Materials and Methods

The remains from Grave 3 were fragmented and commingled. Many of the small hand and foot bones (tarsals, metatarsals, carpals, metacarpals, and phalanges) survived in near perfect condition. All cranial bones were fragmented with few preserved enough to show suture lines. The long bones were fairly fragmented and difficult to identify because only portions of the shafts remained. Many of the remains were subadult therefore, epiphysial ends of some long bones were visible. Only one innominate (Locus 1) was found relatively intact and able to provide a sex and age-at-death estimation.

2.2.1 Minimum Number of Individuals

The MNI technique shows the minimum number of individuals represented in an assemblage (Adams and Konigsberg, 2004; Howard, 1930; Stock, 1929; Vaduveskovic and Djuric, 2019; White, 1953). This minimum number of individuals is represented by the most commonly occurring skeletal element in the assemblage (Vaduveskovic and Djuric, 2019). The number given is the smallest number, not the real or closest value to the real number (Vaduveskovic and Djuric, 2019). The Grave 3 bones could not be sided, unless otherwise noted in parentheses in the text.

When dealing with a commingled assemblage the most important venture is first determining MNI (Vaduveskovic and Djuric, 2019). It is difficult to determine MNI because of the highly fragmentary nature of the remains in this assemblage. For example, there were no complete cranial remains found only small fragments. With all those fragments it is difficult to determine whether they all belonged to one individual or several.

Another technique that is often used when determining the number of individuals in a commingled assemblage is most likely number of individuals (MLNI). MLNI came about out as a modification to the Lincoln Index (LI) used by Adams and Konigsberg (2008) (Osterholtz *et al*., 2014). The MLNI requires pair matching of left and right elements from the same person (Osterholtz *et al*., 2014). This technique can be challenging with poorly preserved skeletal elements (Osterholtz *et al*., 2014).

After consideration of the fragmentary nature of the remains, time constraints due to COVID-19, and MNI being the traditional method (Osterholtz *et al*., 2014; (Vaduveskovic and Djuric, 2019), MNI was chosen for this assemblage to identify the number of individuals.

2.2.2 Sex Estimation

For the purpose of this thesis, 'sex' – meaning male or female – will refer to an individual's genetic makeup and will be evaluated by scoring the pelvic bones, the mandible, and cranial bones.. The scoring methods used in sexing of the skeleton were those found in Buikstra and Ubelaker's (1994) *Standards for Data Collection from Human Skeletal Remains*. The areas of the pelvis that were looked at for scoring were the ventral arc, the subpubic concavity, the ischiopubic ramus ridge and the greater sciatic notch. The cranial morphology used for sexing was the supra-orbital ridge/glabella and the mental eminence.

2.2.3 Age-at-Death Estimation

When estimating the age-at-death of a skeleton, the pubic symphysis, the auricular surface of the ilium, and the cranial sutures are the most commonly used characteristics (Buikstra and Ubelaker, 1994). The standard recording methods used for recording the pubic symphysis were the Todd and Suchey-Brooks methods (Brooks and Suchey, 1990; Buikstra and Ubelaker, 1994; Suchey and Katz, 1986; Todd, 1921a, 1921b).

The auricular surface of the ilium is another common age determination analytical tool. The changes on the auricular surface extend well beyond the age of 50 which, make this method very useful. In addition to this method giving a wider age range, the auricular surface is also more likely to be preserved in forensic and archaeological cases (Lovejoy *et al*., 1985; Meindl and Lovejoy, 1989; White and Folkens, 2005).

Another common method of aging a skeleton is looking at the cranial sutures. *Standards* gives a scoring system based on the degree of suture closure (Baker, 1984; Buikstra and Ubelaker, 1994; Mann et al. 1987; Meindl and Lovejoy, 1985; Todd and Lyon, 1924, 1925a, 1925b, 1925c).

The subadult age-at-death estimations are described in Schaefer, Black and Scheuer's, *Juvenile Osteology* (2009). This provides metric measurements that were used in estimating the age of subadult bones and fusion of epiphyses ends were also taken into consideration. This thesis employed all of these methods when deriving age-at-death estimates from the human remains of Grave 3 at Wadi Faynan.

2.2.4 Paleopathology

Each fragment was examined with identifying signs of pathology in mind. Key pathological identifiers were taken from *Standards for Data Collection from Human Skeletal Remains* (Buikstra and Ubelaker, 1994), *The Human Bone Manual* (White and Folkens, 2005) and *Identification of Pathological Disorders in Human Skeletal Remains* (Ortner, 2003). Studying the pathology left behind on this specific assemblage of remains places emphasis on differential diagnosis that often gets overlooked (Buikstra and Ubelaker, 1994).

The methods used in recording paleopathology in this thesis were observational. The recording of paleopathology was done during the initial inventory process. As Buikstra and Ubelaker (1994) note, "the observer can easily identify and record forms of pathology as the inventory proceeds" (108). Bone abnormalities, that were known to be out of the normal range of variation in healthy individuals, were recorded (Buikstra and Ubelaker, 1994).

2.3 Results

2.3.1 Minimum Number of Individuals

Determining the MNI of this assemblage was done on a Locus-by-Locus basis. Although the remains were separated by Loci, it is not possible to rule out that all or several Loci could have been mixed together. During excavation, the Loci were not clearly distinct and contained some overlap. As a result of the limited analysis time because of COVID-19, cross-checking human remains between Loci was not possible. But, in a separate thesis presented by Julia Tucciarone, the analysis of the teeth from this same assemblage was completed. Tucciarone was able to connect tooth fragments across the Loci within each of the five graves at WF100

(including Grave 3) (Tucciarone, 2020). For the purpose of this thesis, the MNI analysis was done from each individual Loci but it is important to note that overlapping could have occurred.

Grave 3, Locus 1

The fragmentary nature of remains recovered from Locus 1 made estimation of the MNI difficult.

As shown in Table 1, the skeletal elements that contributed to the MNI for adults were: three femoral head fragments. The three femoral heads could not be sided therefore, the lowest MNI for adult individuals would be two.

The skeletal elements that contributed to the subadult MNI calculation were two right ulnae fragments (cannot determine whether they came from the same bone).

Thus, it was determined that Grave 3, Locus 1, contained at least 2 adults and 2 subadults.

Context	**Body Part**	**Skeletal Elements**	
Grave 3, Locus 1	Adult Hand	-13 intermediate phalanges -9 proximal phalanges -5 distal phalanges -3 metacarpals -2 capitate fragments -trapezoid -2 hamate bones (left and right) -2 lunates	
	Adult Foot	-5 intermediate phalange -4 proximal phalange -14 metatarsals	
	Adult Long Bones	-proximal end humeral fragment -humeral distal end -humeral head -left humeral distal end -ulnar proximal epiphysis	-right & left radius -right radius -proximal femur head fragment -2 Femur head fragment -2 tibial proximal epiphyses

	Body Part	Skeletal Elements
	Adult Pelvis	-left and right pelvis came from one individual -fragment of pelvic girdle from older individual
	Adult Thoracic	-left and right clavicle
	Subadult Hand	-3 proximal phalanges -2 distal phalange -1 intermediate phalange -2 unidentified phalanges -left capitate
	Subadult Foot	-right navicular
	Subadult Long Bones	-humeral head -2 proximal epiphyses of humerus -distal epiphysis of humerus -proximal epiphysis of ulna -distal ulnar epiphysis fragment -2 right ulna fragments -radial proximal epiphysis -proximal epiphysis of tibia -proximal end of femur
	Subadult Pelvis	-acetabular of ilium

Table 1: MNI calculation; Locus 1

Grave 3, Locus 2

The bone fragments recovered from Locus 2 (Table 2) were all bones of the hand and foot. The calcanei and cuboid bones that were recovered were too badly damaged to provide a siding. Because of the small number of bones recovered, Locus 2 contained at least one adult individual, as no subadult bones were recovered.

Context	Body Part	Skeletal Element	
Grave 3, Locus 2	Adult Hand	-trapezoid -trapezium	
	Adult Foot	-2 proximal foot phalanges -1 distal foot phalange -4 intermediate foot phalanges -right talus	-navicular -2 calcanei (sides unidentifiable) -2 cuboids (sides unidentifiable) -cuneiform

Table 2: MNI calculation; Locus 2

Grave 3, Locus 3

In Locus 3 (Table 3), there were several hands and feet bones recovered from an adult individual. Noted in the excavation notes, an articulated adult foot was recovered, and an articulated child was also noted and recovered. From the articulated adult foot, four intermediate and three proximal phalanges were identified. Four metatarsal fragments were recovered but, none could provide a side.

Few subadult remains were found to give an accurate MNI calculation.

Thus, it was determined that Grave 3, Locus 3, contained at least 1 adult and 1 subadult.

Context	Body Part	Skeletal Elements
Grave 3, Locus 3	Adult Hand	-2 intermediate phalanges -3 metacarpal fragments
	Adult Foot	-4 intermediate phalanges -3 proximal phalanges -4 metatarsal fragments
	Subadult Skeletal Elements	-right mandible -tibia head fragment -distal hand phalange -lunate

Table 3: MNI calculation; Locus 3

Grave 3, Locus 4

The skeletal element that helped in the calculation of MNI for Locus 4, were the two left capitate bones recovered.

There were no MNI identifying subadult bones recovered.

Based on the two left capitates recovered, Grave 3, Locus 4, contained at least 2 adults and 1 subadult.

Context	Body Part	Skeletal Elements
Grave 3, Locus 4	Adult Hand	-7 intermediate phalanges -3 distal phalange -1 left metacarpal 1 -1 proximal phalange -3 capitates, 2 left -left lunate
	Adult Foot	-2 intermediate phalanges, phalange 1 -1 proximal phalange -1 distal phalange -6 metatarsals
Grave 3, Locus 4	**Body Part**	**Skeletal Elements**
	Subadult Skeletal Elements	-2 vertebrae body fragments -ilium -radial proximal end -distal hand phalange -left scaphoid -distal epiphysis of tibia -proximal end of fibula -right lunate
	Adult Long Bone	-right femur shaft -2 femur head fragments -right humerus -ulna proximal end -left ulna

Table 4: MNI calculation; Locus 4

Grave 3, Locus 5

There were very few bones recovered from Locus 5 (Table 5). Among those bones recovered that help in identifying MNI were two clavicle bones (one identified as a left, the other too fragmented to side).

Thus, it was determined that Grave 3, Locus 5, contained at least 1 adult, as no subadult bones were recovered.

Context	Body Part	Skeletal Elements	
Grave 3, Locus 5	Adult Thoracic	-2 clavicles, one is a left	
	Adult Skull Fragments	-right parietal	-occipital

Table 5: MNI calculation; Locus 5

Grave 3, Locus 6

Once again, very few bones were recovered in Locus 6 to aid in MNI calculations. Thus, it was determined that Grave 3, Locus 6, contained at least 1 adult and 1 subadult.

Context	Body Part	Skeletal Elements
Grave 3, Locus 6	Adult Hand	-1 metacarpal 1 -2 intermediate phalange -1 proximal phalange -1 distal phalange -right trapezoid
Grave 3, Locus 6	**Body Part**	**Skeletal Elements**
	Adult Foot	-7 metatarsal fragments -4 proximal phalanges -1 intermediate phalange -1 distal phalange -left cuneiform
	Adult Skull	-right zygomatic bone -right temporal bone -upper right maxilla fragment, teeth still in situ
	Adult Long Bone	-ulna -2 distal epiphyses of femur -right patella
	Subadult Skeletal Elements	-tibia proximal epiphysis -ulna proximal epiphysis -distal phalange

Table 6: MNI calculation; Locus 6

Grave 3, Locus 99

There was a significant number of bones recovered from Locus 99 (Table 7). Six adult right patellae were recovered and able to give an MNI calculation.

For subadults, six fragmented femur heads were recovered but, were too badly damaged to identify siding.

Thus, based on the six adult right patellae and six subadult femur heads, it was determined that Grave 3, Locus 99, contained at least 6 adults and 3 subadults.

Context	Body Part	Skeletal Element
Grave 3, Locus 99	Adult Hand	-24 metacarpals -32 proximal phalange -45 intermediate phalange -15 distal phalange (one is a distal phalange 1) -left trapezoid -2 left scaphoids -2 left pisiform -1 left trapezoid -1 right hamate
	Adult Foot	-22 metatarsals -19 proximal phalanges -5 intermediate phalanges -4 distal phalanges -5 tali -left navicular -2 calcanei -4 cuneiform
	Adult Skull	-2 occipital bones -frontal bone of the eye orbit -right temporal bone -temporal bone fragment
	Adult Long Bones	-left distal humerus -2 distal end of humerus -left humerus head -4 humerus head -left humerus shaft -right radius shaft -2 right proximal ulna head -right femur head -right medial condyle of femur -6 femur heads -3 femur shaft -intercondylar fossa and condyle of femur -femur distal end fragment
	Adult Exocranial	-6 right patella -4 left patella -3 patella fragments -right scapula -15 vertebrae body fragment -cervical vertebrae -thoracic vertebrae -manubrium -pelvic border

Context	Body Part	Skeletal Elements
Grave 3, Locus 99	Subadult	-right radial proximal end -ulnar head -2 proximal tibia heads -6 femur heads -distal end of femur -distal posterior femur -proximal end of tibia -7 vertebrae body -vertebrae arch -left ischium bone -2 proximal phalange -3 proximal epiphysis of radius -radial head fragment -mandible fragment -talus fragment -left navicular fragment -right scaphoid

Table 7: MNI calculations; Locus 99

In Locus 1, there appears to be two adults and two subadults. Loci 3, 4, and 6 appear to have at least two individuals each, one being an adult and the other being a subadult. Locus 2 and 5 appear to have only one adult individual. The MNI for adult individuals in Locus 99 is six because of the six right patellae that were found. In Locus 99 for subadult, the MNI appears to also be three individuals because of the six femora heads that were found and could not be sided. Therefore, the total MNI that make up this charnel house is 14 adults and 8 subadults.

2.3.2 Sex Estimation

Locus 1

In Locus 1, a right and a left pelvis were found in the same box that it was placed in after excavation. The right side of the pelvic bone was fragmented but some key scoring bones were still intact, allowing for sex estimation by analyzing the ramus ridge, the greater sciatic notch,

and the preauricular sulcus (Table 8). The ventral arc and subpubic concavity were not present to be analyzed but, the greater sciatic notch was scored as a 1/2, the preauricular sulcus was scored as a 3/4, and the ramus ridge was present and narrow. The left side of the pelvic bone was a little more fragmented and was not able to be sexed accurately therefore, was omitted from this analysis.

Locus 1- Right Pelvic Bone	
Ventral Arc	N/A
Subpubic Concavity	N/A
Ramus Ridge	Present, narrow
Greater Sciatic Notch	1 / 2
Preauricular Sulcus	3 / 4

Table 8: Sex estimation for right pelvic bone; Locus 1

For the second fragmented piece of pelvic bone that was found, the greater sciatic notch appears to be male (Table 9), but this conclusion may not be accurate because the other sexing characteristics were not able to be scored thus, potentially skewing the data.

Locus 1- Left Pelvic Bone	
Ventral Arc	N/A
Subpubic Concavity	N/A
Ramus Ridge	N/A
Greater Sciatic Notch	4 / 5
Preauricular Sulcus	N/A

Table 9: Sex estimation for left pelvic bone; Locus 1

A mandible fragment was found in Locus 1 with the mental eminence present. After analyzing the mental eminence, it was scored as a 4/5 (Table 10). The scoring suggests this fragment belonged to a male individual but, without the rest of the skull intact this result does not hold much value.

Locus 1- Mandible Fragment	
Mental Eminence	4 / 5

Table 10: Sex estimation for mental eminence; Locus 1

Locus 2 and Locus 3

No fragments found in Locus 2/3 were able to provide a sexing estimation of the remains.

Locus 4

A pubic bone fragment was also found in Locus 4. The greater sciatic notch was used in determining sex because it was the only area still intact on the fragment. The greater sciatic notch was scored as a 3/4 (Table 11). The score of 3/4 on the greater sciatic notch was too ambiguous to determine whether this fragment belonged to a male or female. Therefore, a sex determination was not able to be provided for this individual.

Locus 4- Left Pelvic Bone	
Ventral Arc	N/A
Subpubic Concavity	N/A
Ramus Ridge	N/A
Greater Sciatic Notch	3 / 4
Preauricular Sulcus	N/A

Table 11: Sex estimation for left pelvic bone; Locus 4

Locus 5, Locus 6 and Locus 99

No fragments of the remains found in Locus 5, 6 and 99 were able to provide sexing estimation. Therefore, in total, 1 female and 2 males were able to be identified in this charnel house.

2.3.3 Age-at-Death Estimation

Adult

The bones that were looked at for estimating age-at-death in this assemblage were those that were able to provide an actual age range by looking at the public symphysis or auricular surface that was visible (Table 12). The young adult pubic symphysis has a rugged surface bearing horizonal ridges and intervening grooves (White and Folkens, 2005). The surface loses relief with age and is bounded by a rim by age 35 (White and Folkens, 2005). Subsequent erosion and general deterioration progress after this age allowing the osteologist to determine whether or not the person had been an older individual (White and Folkens, 2005).

In Locus 1, an auricular surface was present that was able to provide an age range of 35-40 years because of its similarity to the images in Phase 4/5 of *The Human Bone Manual* (White and Folkens, 2005). A right pelvis was also found in Locus 1, and the pubic symphysis was able to give an age-at-death estimation of around 22-26 after scoring a 2/3 on both Todd's and Suchey-Brooks methods.

In Locus 4, a left pelvis with the auricular surface visible showed that this individual was around 36-38 years old at time of death because of its similarities to Phase 4 in *The Human Bone Manual* (White and Folkens, 2005).

Adult Age-at-Death					
Context	**Skeletal Element**	**Age Estimation**	**Todd Method**	**Suchey-Brooks Method**	**Auricular Surface**
Grave 3, Locus 1	Auricular Surface	35-40 years			Phase 4/5
	Right Pelvis-Pubic Symphysis	22-26 years	2/3	2/3	

Context	Skeletal Element	Age Estimation	Todd Method	Suchey-Brooks Method	Auricular Surface
Grave 3, Locus 4	Left Pelvis-Auricular Surface	36-38 years			Phase 4

Table 12: Adult Age-at-Death; Loci 1, 4

Subadult

In Locus 4 (Table 13), an ilium was found that was estimated to be around 2-5 years because of its measurement for maximum iliac length of 58.10mm and using Molleson and Cox's metric scoring in *Juvenile Osteology* (2009) as a reference (Molleson and Cox, 1993; Schaefer *et al*., 2009).

In Locus 99 (Table 13), the base of a proximal phalange was able to provide an age estimation of around 12-14 years because of a sharp medial border and, a blunt lateral border (Birkner, 1978; Fazekas and Kósa, 1978; Garn *et al*., 1967; Garn *et al*., 1975; Plato et al., 1984; Schaefer *et al*., 2009). A left ischium was also recovered belonging to an infant around 6 months to a year old, based on the descriptions in Molleson and Cox (1993) and White, Black and Folkens (2012). Two femur heads were found with blunt projections on their metaphyseal surfaces, one was 8 years or younger, and the other was approximately 3 years or younger because there was no margin present (Elgenmark, 1946; Fazekas and Kósa, 1978; Garn *et al*., 1967; McKern *et al*., 1957; Schaefer *et al*., 2009). A vertebrae body fragment was identified to be approximately 6 years with a grooved surface (Albert et al., 1995; Bagnall *et al*., 1977; Fazekas and Kósa, 1978; McKern *et al*., 1957; Schaefer *et al*., 2009). The proximal epiphysis of the radius was found and estimated to be approximately 10 years old because of the present fovea which develops around the age of 10 (Elgenmark, 1946; Fazekas and Kósa, 1978; Garn *et*

al., 1967; Ghantus, 1951; Gindhart, 1973; Jeanty, 1983; Maresh, 1970; Schaefer, 2008; Schaefer *et al*., 2009; Scheuer *et al*., 1980;).

Subadult Age-at-Death			
Context	**Skeletal Element**	**Age Estimation**	**Reason**
Grave 3 Locus 4	Ilium	2-5 years	Molleson and Cox (1993)
Grave 3, Locus 99	Base of proximal phalange	Approx. 12-14 years	Sharp medial border, blunt lateral border
	Left ischium	6 months- 1 year old	Molleson and Cox (1993), White, Black and Folkens (2012)
	Femur head	Approx. 8 years or younger	Blunt projection
	Femur head	Approx. 3 years or younger	Blunt projection
	Vertebrae body fragment	Approx. 6 years	Grooved surface
	Proximal epiphysis of radius	Approx. 10 years	Fovea present

Table 13: Subadult Age-at-Death; Loci 4, 99

2.3.4 Paleopathology

Most of the skeletal elements bearing pathology in Grave 3 were phalanges of the hands and foot, and two vertebral bodies (one identified as a lumbar). The results of the inventory are shown in the table below (Table 14). Two phalanges (Locus 1 and Locus 99) appear to have a bony growth on the proximal base (Figures 3 & 4), which could be attributed to osteoarthritis. Osteoarthritis is also present on the vertebrae (Figures 8 & 9) in the form of bony spurs forming vertically on the superior surface of the vertebrae. The bony growth shown on both these phalanges from Loci 1 and 99 appear to be similar in nature as occurring on the side of the phalange at the base. These phalanges were found in different Loci, but because the grave had a

lot of disturbance, particularly at the eastern end, between the loci, it cannot be ruled out that these two phalanges could have come from the same individual. Several of the phalanges had striation marks on the lateral and anterior surfaces which could be signs of enlarged muscle attachments (the striation marks are show in Figures 5-7).

Osteoarthritis (Degenerative Joint Disease) is a disease that will often show up on bones and is the most common form of arthritis. Osteoarthritis can be seen in the two vertebrae fragments of this assemblage and in the phalanges in Loci 1 and 99. Osteoarthritis will affect the areas of the cervical and lumbar regions of the vertebrae (Waldron, 2009). This can be proved in the lumbar vertebrae (Figure 9) where the osteoarthritis is showed. The vertebral fragments that showed signs of osteoarthritis in this assemblage could not be aged or sexed because of the commingled nature, it cannot be known whether or not they were older individuals, what their sex was, or whether or not they suffered trauma in their life. In regards to the hand, osteoarthritis is common in areas such as the distal and proximal interphalangeal joints (dips) and (pips) (Waldron, 2009). The phalanges in Loci 1 and 99 appear to exhibit the bony growth at the base and between phalanges.

Osteoarthritis occurs mostly in load-bearing joints such as, the spine, hip and knees (Matt *et al*., 1995; White and Folkens, 2005). This disease may affect a single joint (monoarticular) or many joints (polyarticular) and there may be a great production of new bone (hypertrophic), or very little (atrophic) (Waldron, 2009). Based on the bony growth on the phalanges and the bony spurs on the vertebrae, it appears this osteoarthritis is hypertrophic in nature. The patterns of osteoarthritic lesions of an individual (or population level) can shed light on prehistoric activity patterns (Listi *et al*., 2012; White and Folkens, 2005). This disease is the destruction of cartilage in the joint which can be a result of repetitive motion. A normal joint is

able to withstand physiological loads but, abnormal loading can increase the risk of osteoarthritis (Roach and Tilley, 2007).

The enlarged muscle attachments shown on the proximal and intermediate hand phalanges and the proximal foot phalange could also be the result of osteoarthritis caused by repetitive motion. The muscles that attach to the proximal phalanges are the lumbricals (medial aspect of the four lateral phalanges) and the interossei (both sides of the second, third and fourth proximal phalanges) (O'Leary, 2020). There are several muscles that attach to the proximal hand phalanges which include the posterior (extensor) forearm muscles, the metacarpal muscles, the thenar muscles and the hypothenar muscles (Rad, 2020). The intermediate phalanges are less mobile compared to the proximal phalanges (Rad, 2020), which is interesting considering that the enlarged muscle attachment appeared on two of the intermediate phalanges. The only muscle that attaches to the intermediate phalanges are the flexor digitorum superficialis muscle, which attaches to the sides of the phalanges and allows them to flex at the PIP joints (Rad, 2020). Touraine *et al*. (2014) notes that short bone spurs may be visible on the tendon insertions on the lateral sides of the proximal phalanges, these are just normal variants and are not clinical in nature.

Although these remains were fragmentary in nature, several pathological indicators could be drawn from them. Osteoarthritis is seen on the phalanges in Loci 1 and 99, on the vertebrae and, the enlarged muscle attachments show that these individuals were doing laborious work. These individuals were mining and farming and processing ore, which are all very difficult and strenuous tasks (Adams, 2002, 2006; Adams and Dolphin, 2019; Adams et al., 2019). The continued activity every day shows up on the bones of these individuals in the form of osteoarthritis. Assessing pathology also gives an insight into the daily life of these individuals.

Context	Skeletal Element	Pathology	Description
Grave 3 Locus 1	Phalange	Phalangeal Exostosis	Bony growth on side of phalange
Grave 3 Locus 4	Left metacarpal 1	Unidentified	Enlarged muscle attachment on medial and lateral sides – seen both posteriorly and anteriorly
Grave 3 Locus 99	Proximal hand phalange	Unidentified	Enlarged muscle attachment on medial and lateral sides as seen more prominently anteriorly
	Proximal foot phalange	Unidentified	Enlarged muscle attachment on medial and lateral sides – seen both posteriorly and anteriorly
	Intermediate hand phalange	Unidentified	Enlarged muscle attachment on medial and lateral sides as seen more prominently posteriorly
	Intermediate hand phalange	Phalangeal Exostosis	Bony growth on side of phalange
	Vertebrae body fragment	Osteoarthritis	Bony growth visible when viewing the fragment superiorly
	Vertebrae body	Osteoarthritis	Bony growth visible on superior edge of the vertebrae body

Table 14: Pathology for Loci, 1, 4, 99

Figure 3: *Bony growth, Locus 1- phalange, posterior, adult*

Figure 4: *Bony growth, Locus 99- phalange, lateral, adult*

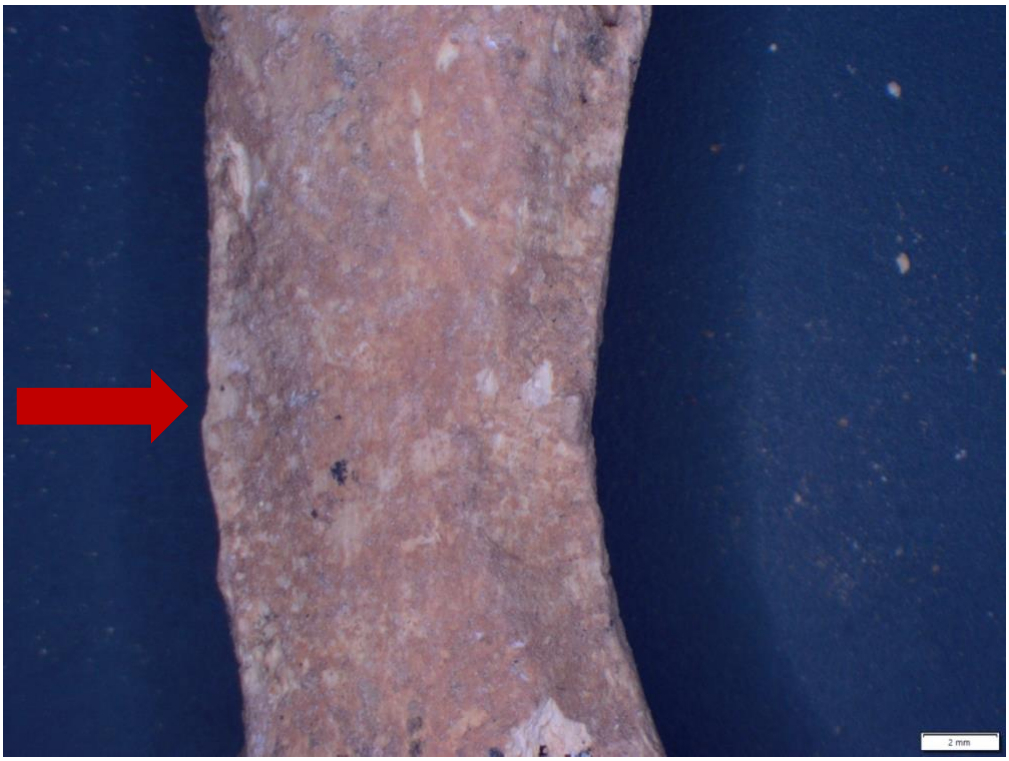

Figure 5: *Enlarged muscle attachment, anterior, Locus 4- left metacarpal 1, anterior, adult*

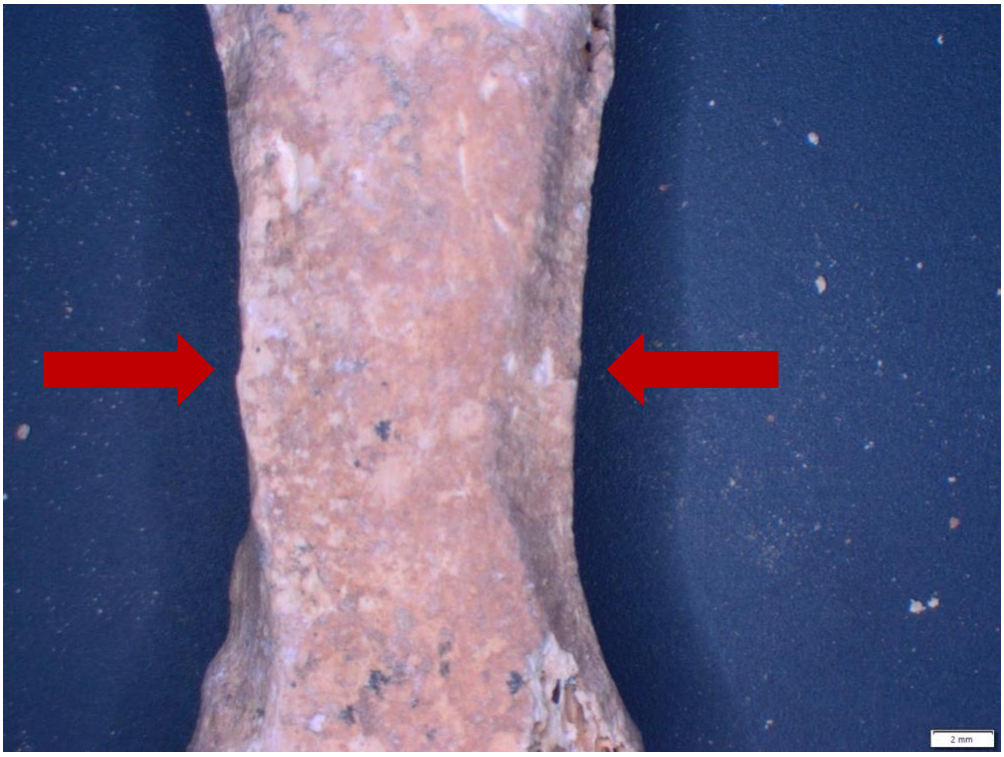

Figure 6: *Enlarged muscle attachment, anterior, Locus 4- left metacarpal 1, posterior, adult*

Figure 7: *Enlarged muscle attachment, anterior, Locus 4- left metacarpal 1, medial, adult*

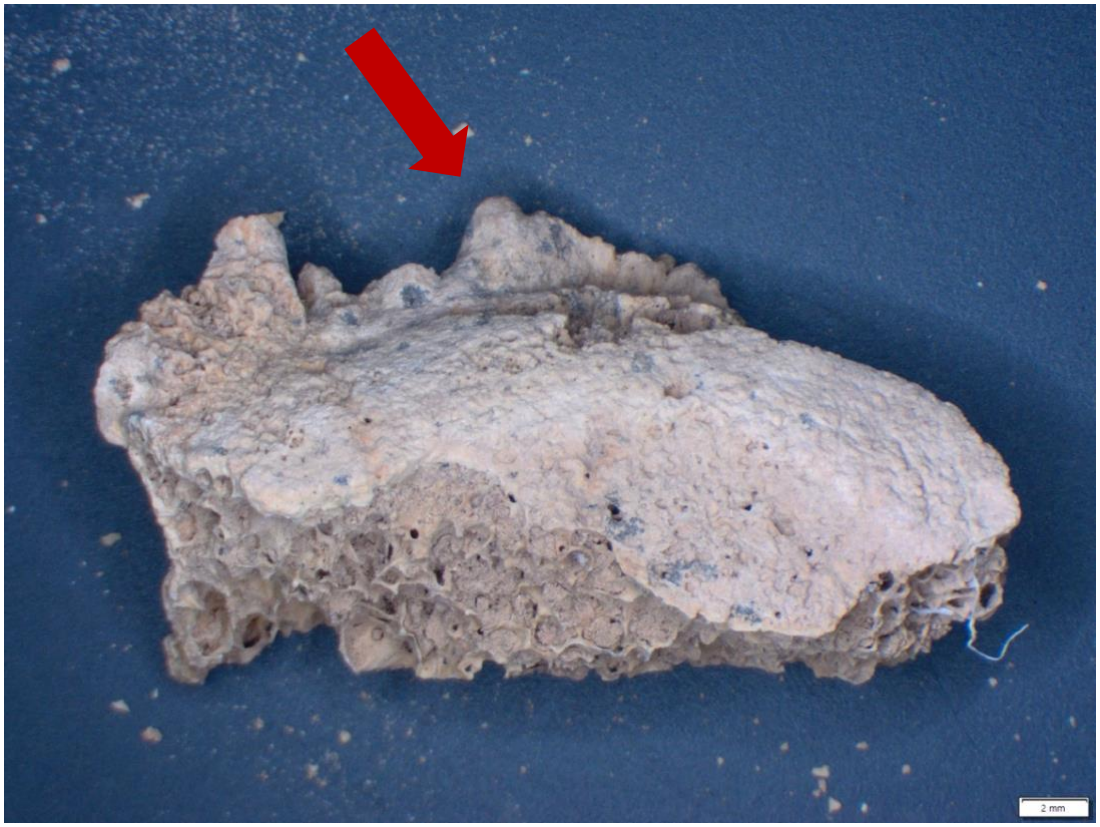

Figure 8: *Osteoarthritis, Locus 99- vertebrae body fragment, superior, adult*

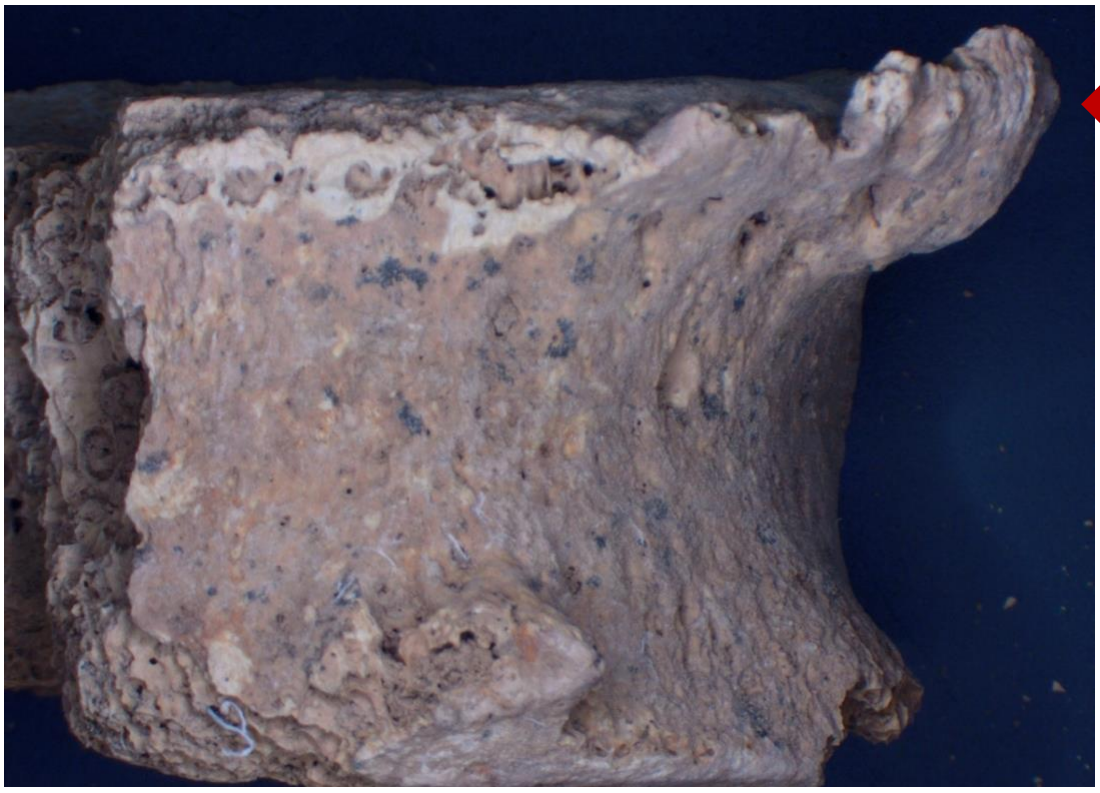

Figure 9: *Osteoarthritis, Locus 99- lumbar vertebrae body, lateral, adult*

2.4 Discussion

The traditional osteological methods used in this thesis provide a preliminary look into the individuals at WF100. WF100 is a heavily looted burial site (Adams and Dolphin, 2019) and thus makes a traditional osteobiography of the skeletal assemblage difficult. The MNI of this specific charnel house is only a glance into the numerous people buried at this site, but it is a start. Comparing the MNI of Grave 3 at WF100, 22 individuals – including adults and subadults – to Bab edh-Dhra, where one to 37 individuals were found in the shaft tombs (Ortner and Frohlich, 2007; Ullinger *et al*., 2012). Chesson (1999) notes that the charnel houses found at Bab edh-Dhra had an even greater number of individuals than the shaft tombs, which may represent larger kinship relationships (Chesson, 1999; Rast and Schaub, 1979). Working with such a highly fragmentary and commingled assemblage such as this one can make determining MNI difficult. Basing MNI off the known number of skeletal elements humans have (e.g., six right adult patellae in Locus 99) is a good start to knowing how many adult individuals were buried in Grave 3, but there is still a level of uncertainty. Presumably, the act(s) of looting over time removed other individuals from their resting place in Grave 3, but we can at least identify the presence of twenty-two individuals (adult and subadults included). This is further proved in the age overlaps occurring within subadult individuals and knowing that the Loci may not have been all distinct. Some of the subadult bones that had age overlaps could have belonged to the same individual.

Providing sex estimations for skeletal remains is important for the biological profile of an individual or a group of individuals such as those at WF100. Sex estimation and assessment can help answer questions on cultural variation in behaviour that is preserved in the functional adaptations of the skeleton (DiGangi and Moore, 2013; Sheridan, 2017).

Sex estimates for the individuals of Grave 3 was limited by the fragmentary nature of these remains, where very few sex characteristics are noted because key sex identifying elements are broken. The pubic symphysis and auricular surface of the ilium were analyzed to provide an age-at-death estimation. The age range of adults in the assemblage was between 20-40 years of age. There were no intact skulls found, therefore, it made it difficult to estimate age-at-death based on cranial suture closures. As a result of this, cranial suture closures were not used in this analysis to aid in identifying specific age-at-death but, where cranial sutures were noted and able to be identified, they are noted in the basic inventory of the entire assemblage.

With regard to subadult bone fragments, it is relatively easy to know when a fragment is from a subadult human based on the thickness of the bone, while determining more specific age-at-death estimates is made possible through observation of the fusion of the epiphyses of the bones given that they fuse within a known age range (White and Folkens, 2005). The age range for the subadults in this assemblage was around 6months-14 years of age. There are, of course, limits to estimating age based on epiphyseal unions. In females, the union begins earlier than it does in males which means that different individuals of the same sex can show different times of union (White and Folkens, 2005).

Many of the subadult fragments in this assemblage were only table to be labelled ‘subadult’ because of the absence of fusion, very few provided a range of age. Measurements can be able to estimate the age of the subadult but, with a highly fragmented assemblage such as this one, it was difficult to take measurements. Therefore, only measurements where the bones were fully intact were taken and used in the age-at-death estimations.

The sex and age-at-death estimations show that both males and females were buried in the charnel house and the age range was between 6months-40 years of age. This is similar to Bab

edh-Dhra where there were no selective burials and men, women, and children were all interred together (Gregoricka *et al*., 2019). From a simple osteological analysis, such as the one in this thesis, it is difficult to tell whether or not the individuals were part of the same kinship group or not but, hopefully that will pave the way for future research at this site.

The paleopathology noted on the remains could be due to daily repetitive activities which lead to skeletal modifications (Ullinger *et al*., 2012). Similar to Bab edh-Dhra, where the individuals were constructing shaft tombs and unique ceramics, it can be presumed that these tasks were also being done at WF100. The tasks (for example, mining, smelting, processing ore, farming, constructing the tombs, etc.), (Adams, 2002, 2006; Adams and Dolphin, 2019; Adams et al., 2019), being done at WF100 could have led to the osteoarthritis shown on the vertebrae and phalanges. The striation marks observed on several phalanges could be the result of enlarged muscle attachments based off the daily work that these individuals would have been doing.

2.5 Conclusions

This thesis is presented as a preliminary assessment of the individuals that were found at Wadi Faynan 100 during the Barqa Landscape Project in 2019. This thesis helps to further prove what has already been discovered at Bab edh-Dhra, that men, women and children were interred together with varying age ranges. These individuals were also doing significant repetitive motion that was able to be seen as a skeletal modification on the phalanges of the individuals.

The remains that were analyzed were highly fragmented and commingled which made the analysis, at times, fairly difficult. That, coupled with the time constraints due to COVID-19, made it difficult to be able to go into further analysis of the remains, such as non-metric traits, further analysis into paleopathology, etc.

The aim of this research is that it can be referenced in the future for other remains found at WF100 or in other areas of Jordan. The hope is that this research can further be used as part of a larger analysis done on the all the remains found at WF100, including the remains found in Graves 1, 2, 4, and 5.

3.1 Bibliography

Adams, B.J. and Konigsberg, L.W. (2004). How many people? Determining the number of individuals represented by commingled human remains. In: Adams, B.J., editor. Recovery, analysis, and identification of commingled human remains. *Totowa*: Humana Press; p.241-55

Adams, R., & Dolphin, A. (2019). Barqa Landscape Project. *Archaeology in Jordan*; p.136-138

Adams, R. (1999). "The development of copper metallurgy during the Early Bronze Age of the Southern Levant: Evidence from the Faynan region, Southern Jordan." Unpublished PhD thesis, Sheffield University.

- (2000). "The EBA III–IV transition in southern Jordan: Evidence from Khirbet Hamra Ifdan." In *Ceramics and Change in the Early Bronze Age of the Southern Levant*, edited by G. Philip and D. Baird, 379–401. Levantine Archaeology 2. Sheffield: Sheffield Academic Press.
- (2002). "From farms to factories: The development of copper production at Faynan, southern Jordan, during the Early Bronze Age." In *Metals and Society*, edited by B. S. Ottaway and E. C. Wagner, 21–32. British Archaeological Reports, International Series. Oxford: Archaeopress.
- (2006). "Copper trading networks across the Arabah during the later Early Bronze Age." In *Cross- ing the Rift: Resources, Routes, Settlement Patterns and Interaction in the Wadi Arabah*, edited by P. Bien- kowski and K. Galor, 135–142. Oxford: Oxford University Press.
- (2008). Archaeology in Jordan: A Brief History, 1–6.
- (2020). Personal communication.

Adams, R., Dolphin, A., Grattan, J., Haylock, K., Thebes, J., Weston, A., Meijer, J., Lawson, A., and Harris, A. (2019). Barqa Landscape Project 2019: Preliminary Report to the Department of Antiquities, 1-20

Adams, R. B. and H. Genz. (1995). "Excavations at Wadi Fidan 4: A Chalcolithic village complex in the Cop- per ore district of Feinan, southern Jordan." *Palestine Exploration Quarterly* 127: 8–20.

Albert, A.M. and Maples, W.R. (1995). Stages of epiphyseal union for thoracic and lumbar vertebral centra as a method of age determination for teenage and young adult skeletons. Journal of Forensic Sciences 40(4): 623–633.

Bagnall, K.M., Harris, P.F., and Jones, P.R.M. (1977). A radiographic study of the human fetal spine. 2. The sequence of development of ossification centers in the vertebral column. Journal of Anatomy 124(3): 791–802.

Barker, A. W. (2018). Looting, the Antiquities Trade, and Competing Valuations of the Past. *Annual Review of Anthropology*, 47(1), 455–474.

Barker, G., Creighton, O., El-Rishi, H., Gilbertson, D., Grattan, J., Hunt, C., . . . Reynolds, T. (2007). Chalcolithic (c. 5000-3600 cal. BC) and Bronze Age (c.3600-1200 cal. BC) settlement in Wadi Faynan: Metallurgy and Social Complexity. In 1017661475 782377946 R. Adams (Ed.), *Archaeology and Desertification*.

Barker G., Gilbertson D. and Mattingly D. (eds.). 2007. A*rchaeology and Desertification. The Wadi Faynan Landscape Survey, Southern Jordan*. Oxford: Oxbow Books.

Birkner, R. (1978). Normal Radiographic Patterns and Variances of the Human Skeleton – An X-ray Atlas of Adults and Children. Baltimore (Munich): Urban and Schwarzenberg.

Blythe, A., & Bowman, B. (2018). Field archaeologists as Eyewitnesses to Site Looting. *Arts, 7*(3), 1-24.

Brodie, N. (2015). Syria and its Regional Neighbors: A Case of Cultural Property Protection Policy Failure? *International Journal of Cultural Property*, 22(2-3), 317–335.

Brooks, S. T. and Suchey, J. M. (1990). Skeletal Age Determination Based on the Os Pubis: A Comparison of the Acsádi-Nemeskéri and Suchey-Brooks Methods. *Human Evolution* 5:227-238.

Buikstra, J. E., & Ubelaker, D. H. (1994). *Standards for data collection from human skeletal remains*. Arkansas Archeological Survey.

Chesson, M. S. (1999). "Libraries of the Dead: Early Bronze Age Charnel Houses and Social Identity at Urban Bab Edh-Dhra, Jordan." *Journal of Anthropological Archaeology* 18, no. 2: 137–64.

Chesson, M. S. (2001). Embodied Memories of Place and People: Death and Society in an Early Urban Community. *Archeological Papers of the American Anthropological Association*, 10(1), 100–113.

Department of Antiquity: Projects. (2019). Retrieved 2020, from http://doa.gov.jo/Projectsen.aspx

DiGangi, E. A., & Moore, M. K. (2013). *Research methods in human skeletal biology*. Amsterdam: Elsevier Academic.

Edge, S. (1991). "Jordan's Fate Hangs in the Balance." *MEED Middle East Economic Digest*, p. 1-3.

Elgenmark, O. (1946). The normal development of the ossific centres during infancy and childhood. Acta Paediatrica Scandinavica 33(Suppl. 1).

Fabiani, M. (2018). Disentangling Strategic and Opportunistic Looting: The Relationship between Antiquities Looting and Armed Conflict in Egypt. Arts (Basel), 7(2), 22, p. 1-26.

Fazekas, I.Gy. and Ko´sa, F. (1978). *Forensic Fetal Osteology*. Budapest: Akade´miai Kiado´.

Feitelson, E., Tamimi, A., & Rosenthal, G. (2012). Climate change and security in the Israeli–Palestinian context. *Journal of Peace Research*, 49(1), 241–257.

Garn, S.M., Burdi, A.R., Babler, W.J., and Stinson, S. (1975). Early prenatal attainment of adult metacarpal- phalangeal rankings and proportions. American Journal of Physical Anthropology 43: 327–332.

Garn, S.M., Rohmann, C.G., and Silverman, F.N. (1967). Radiographic standards for postnatal ossification and tooth calcification. Medical Radiography and Photography 43: 45–66.

Ghantus, M. (1951). Growth of the shaft of the human radius and ulna during the first two years of life. American Journal of Roentgenology 65: 784–786.

Gindhart, P. (1973). Growth standards for the tibia and radius in children aged one month through eighteen years. American Journal of Physical Anthropology 39: 41–48.

Gregoricka, L., Ullinger, J., & Sheridan, S. (2019). Status, kinship, and place of burial at Early Bronze Age Bab adh-Dhra': A biogeochemical comparison of charnel house human remains. *American Journal of Physical Anthropology*, p. 319-335.

Haija, A. A. A. (2011). Jordan: Tourism and conflict with local communities. *Habitat International*, 35(1), 93–100.

Howard, H. (1930). A census of the Pleistocene birds of Rancho La Brea from the collections of the Los Angeles Museum. *Condor*. 32:255-271

Hsieh, S. (2018). The Charitable Deduction and Looting of Antiquities: A Comparative Approach. *Cornell International Law Journal*, *51*(2), p. 471-493.

International Journal of Osteoarchaeology. (n.d.). Retrieved from https://onlinelibrary.wiley.com/page/journal/10991212/homepage/productinformation.html

Jeanty, P. (1983). Fetal limb biometry. (Letter). Radiology 147: 601–602.

Lapp, P. W. (1968). Bâb edh-Dhrâ Tomb a 76 and Early Bronze I in Palestine. *Bulletin of the American Schools of Oriental Research*, 189, 12–41.

Levy, T. E., R. B. Adams, A. Hauptmann, M. Prange, S. Schmitt-Strecker and M. Najjar. (2002). “Early Bronze Age metallurgy: A newly discovered copper manufactory in southern Jordan. *Antiquity* 76: 425–437.

Listi, G., & Manhein, M. (2012). The Use of Vertebral Osteoarthritis and Osteophytosis in Age Estimation: AGE ESTIMATION FROM THE VERTEBRAE. Journal of Forensic Sciences, 57(6), 1537–1540.

Lovejoy, C. O., Meindl, R. S., Pryzbeck, T. R., Mensforth, R. P. (1985). Chronological Metamorphosis of the Auricular Surface of the Ilium: A New Method for the Determination of Age at Death. *American Journal of Physical Anthropology* 68:15-28.

Lundén, S. (2012). Perspectives on Looting, The Illicit Antiquities Trade, Art and Heritage. *Art Antiquity and Law.* P. 109-134.

Mann, R. W., Symes, S. A., Bass, W. M. (1987). Maxillary Suture Obliteration: Aging the Human Skeleton Based on Intact or Fragmentary Maxilla. *Journal of Forensic Sciences* 32:148-157

Maresh, M.M. (1970). Measurements from roentgenograms. In: Human Growth and Development (R.W. McCammon, Ed.), pp. 157–200. Springfield IL: C.C. Thomas.

McKern, T.W. and Stewart, T.D. (1957). Skeletal age changes in young American males, analysed from the standpoint of age identification. Headquarters Quartermaster Research and Development Command, Technical Report. EP-45. Natick, MA.

Meindl, R. S., Lovejoy, C. O. (1989). Age Changes in the Pelvis: Implications for Paleodemography. In Age Markers in the Human Skeleton, edited by M. Y. Iscan, pp. 137-168. Charles C. Thomas, Springfield, Illinois.

Molleson, T. and Cox, M. (1993). *The Spitalfields Project Volume 2 – The Anthropology – The Middling Sort,* Research Report 86. London: Council for British Archaeology.

Newnham, D. (1996). Storm in a Dipper Cup. *Home & Gardens*, 70-72.

O'Leary, C. (2020). Phalanges of the foot. Retrieved from https://www.kenhub.com/en/library/anatomy/phalanges-of-the-foot

Ortner, D. J. (2003). *Identification of Pathological Disorders in Human Skeletal Remains*. San Diego, CA: Academic Press.

Ortner, D. J., & Frohlich, B. (2007). The EB IA tombs and burials of Bâb edh-Dhrâ, Jordan: a bioarchaeological perspective on the people. *International Journal of Osteoarchaeology*, 17(4), 358–368.

Osterholtz, A. J., Baustian, K. M., Martin, D. L., & Potts, D. T. (2014). Commingled Human Skeletal Assemblages: Integrative Techniques in Determination of the MNI/MNE. In *Commingled and Disarticulated Human Remains: Working Toward Improved Theory, Method, and Data*. New York: Springer, p. 35-50.

Philip, G. (2008). The Early Bronze Age I-III. *Jordan*, p. 161-226.

Plato, C.C., Greulich, W.W., Garruto, R.M., and Yanagihara, R. (1984). Cortical bone loss and measurements of the second metacarpal bone: II. Hypodense bone in postwar Guamanian children. American Journal of Physical Anthropology 63: 57–63.

Polcaro, A., Muñiz, J., Alvarez, V., & Mogliazza, S. (2014). Dolmen 317 and Its Hidden Burial: An Early Bronze Age I Megalithic Tomb from Jebel al-Mutawwaq (Jordan). *The American Schools of Oriental Research*, 372, 1–17.

Rad, A. (2020). Phalanges of the hand. Retrieved from https://www.kenhub.com/en/library/anatomy/the-phalanges

Rast, W. E., & , R. T. (1979). The Southeastern Dead Sea Plain Expedition: An Interim Report of the 1977 Season. *The Annual of the American Schools of Oriental Research*, 46.

Roach, H., & Tilley, S. (2007). The Pathogenesis of Osteoarthritis. In 1253037377 927821684 M. C. Farach-Carson & 1253037378 927821684 F. Bronner (Eds.), *Bone and Osteoarthritis* (Vol. 4, pp. 1-18). London: Springer-Verlag London Limited.

Roberts, C. (2007). The Human Bones. In 976191037 756957386 S. J. Mithen & 976191038 756957386 B. Finlayson (Authors), *The early prehistory of Wadi Faynan, Southern Jordan: Archaeological survey of Wadis Faynan, Ghuwayr and al-Bustan and evaluation of the pre-pottery Neolithic a site of Wf16*. Oxford: Oxbow.

Rodríguez Temiño, I., Yates, D., Deckers, P., Tantaleán, H., Ulst, I., Sánchez Nava, P., & Musteata, S. (2017). The looting of archaeological heritage (Part 1). AP (Madrid), 3, 5–45.

Schaefer, M. (2008). A summary of epiphyseal union timings in Bosnian males. International Journal of Osteoarchaeol- ogy, DOI: 10.1002/oa.959. Copyright John Wiley & Sons Limited. Reproduced with permission.

Schaefer, M., Black, S., & Scheuer, L. (2009). *Juvenile Osteology*. Elsevier.

Scheuer, J.L, Musgrave, J.H., and Evans, S.P. (1980). The estimation of late fetal and perinatal age from limb bone length by linear and logarithmic regression. Annals of Human Biology 7(3): 257–265.

Sheridan, S. G. (2017). "Bioarchaeology in the Ancient Near East: Challenges and Future Directions for the Southern Levant." *American Journal of Physical Anthropology*, p. 110-152.

Steele, C. S. (1990). Early Bronze Age Socio-Political Organization in Southwestern Jordan. *Zeitschrift Des Deutschen Paldstina-Verein*, 106.

Stock, C. (1929). A census of the Pleistocene mammals of Rando La Brea, based on the collections of the Los Angeles Museum. *J Mammal*. 10:218-9

Suchey, J. and Katz, D. (1986). Skeletal Age Standards Derived from an Extensive Multiracial Sample of Modern Americans. Abstract. *American Journal of Physical Anthropology* 69:269.

Todd, T. W. (1921a). Age Changes in the Pubic Bone. I: The Male White Pubis. *American Journal of Physical Anthropology* 3:285-334.

Todd, T. W. (1921b). Age Changes in the Pubic Bone. III: The Pubis of the White Female. IV: The Pubis of the Female White-Negro Hybrid. *American Journal of Physical Anthropology* 4:1-70.

Todd, T. W., and Lyon, D. W. (1924). Endocranial Suture Closure, Its Progress and Age Relationship. Part I. Adult Males of White Stock. *American Journal of Physical Anthropology* 7:325-384.

Todd, T. W., and Lyon, D. W. (1925a). Cranial Suture Closure, Its Progress and Age Relationship. Part II. Ectocranial Closure in Adult Males of White Stock. *American Journal of Physical Anthropology* 8:23-45.

Todd, T. W., and Lyon, D. W. (1925b). Cranial Suture Closure, Its Progress and Age Relationship. Part III. Endocranial Closure in Adult Males of Negro Stock. *American Journal of Physical Anthropology* 8:47-71.

Todd, T. W., and Lyon, D. W. (1925c). Cranial Suture Closure, Its Progress and Age Relationship. Part IV. Ectocranial Closure in Adult Males of Negro Stock. *American Journal of Physical Anthropology* 8:149-168.

Touraine, S., Wybier, M., Sibileau, E., Genah, I., Petrover, D., Parlier-Cuau, C., Bousson, V., Laredo, J. (2014). Non-traumatic calcifications/ossifications of the bone surface and soft tissues of the wrist, hand and fingers: A diagnostic approach. *Diagnostic and Interventional Imaging, 95*(11), 1035-1044.

Tucciarone, J. (2020). *A Comprehensive analysis of Dental Remains from the Early Bronze Age I site of Wadi Faynan 100, Jordan*. University of Waterloo.

Tucciarone, J. (2020). Personal communication.

Ullinger, J. M., Sheridan, S. G., & Ortner, D. J. (2012). Daily Activity and Lower Limb Modification at Bab edh-Dhrȧ, Jordan, in the Early Bronze Age. *Bioarchaeology and Behavior*, 180-202.

Ulph, J. (2011). "The Impact of the Criminal Law and Money Laundering Measures upon the Illicit Trade in Art and Antiquities." *Art Antiquity & Law* 16, p. 39-52.

Waldron, T. (2009). *Palaeopathology*. Cambridge, New York: Cambridge University Press.

White, T.E. (1953). A method of calculating the dietary percentage of various food animals utilized by aboriginal peoples. *American Antiquity*, 4: 396-8.

White, T. D., Black, M. T., & Folkens, P. A. (2012). *Human osteology*. San Diego, CA: Academic Press.

White, T. D., & Folkens, P. A. (2005). *The Human Bone Manual*. Amsterdam: Elsevier Academic.

Wright, K., Najjar, M., Last, J., Moloney, N., Flender, M., Gower, J., … Shafiq, R. (1998). The Wadi Faynan Fourth and Third Millennia Project, 1997: Report on the First Season of Test Excavations at Wadi Faynan 100. *Levant*, 30(1), 33–60.

Appendix A: Sex Estimation Indicators

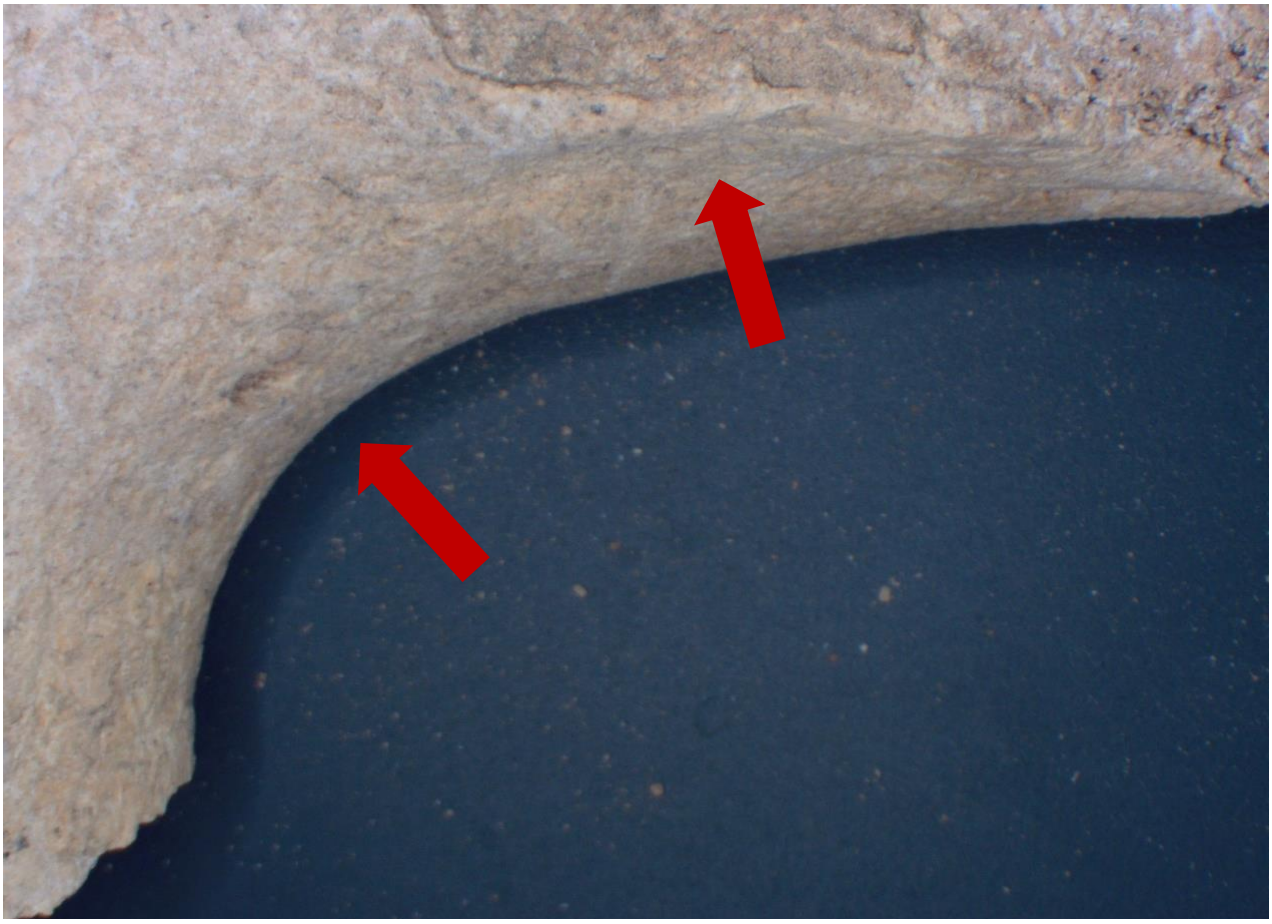

Figure A.1: Preauricular sulcus & greater sciatic notch view, Locus 1- right pelvis, anterior, adult

Figure A.2: Ramus ridge, Locus 1- right pelvis, anterior, adult

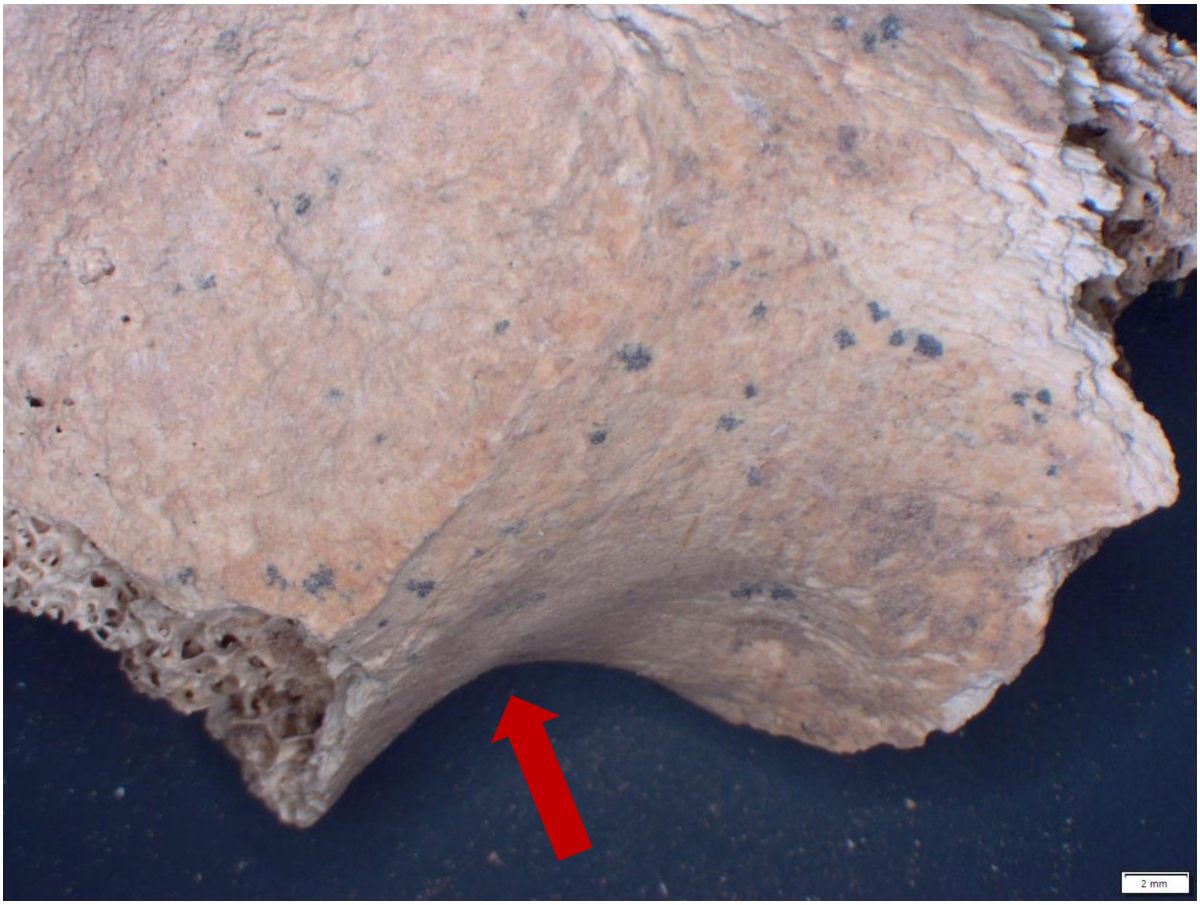

Figure A.3: Greater sciatic notch, Locus 1- left pelvis, medial, adult

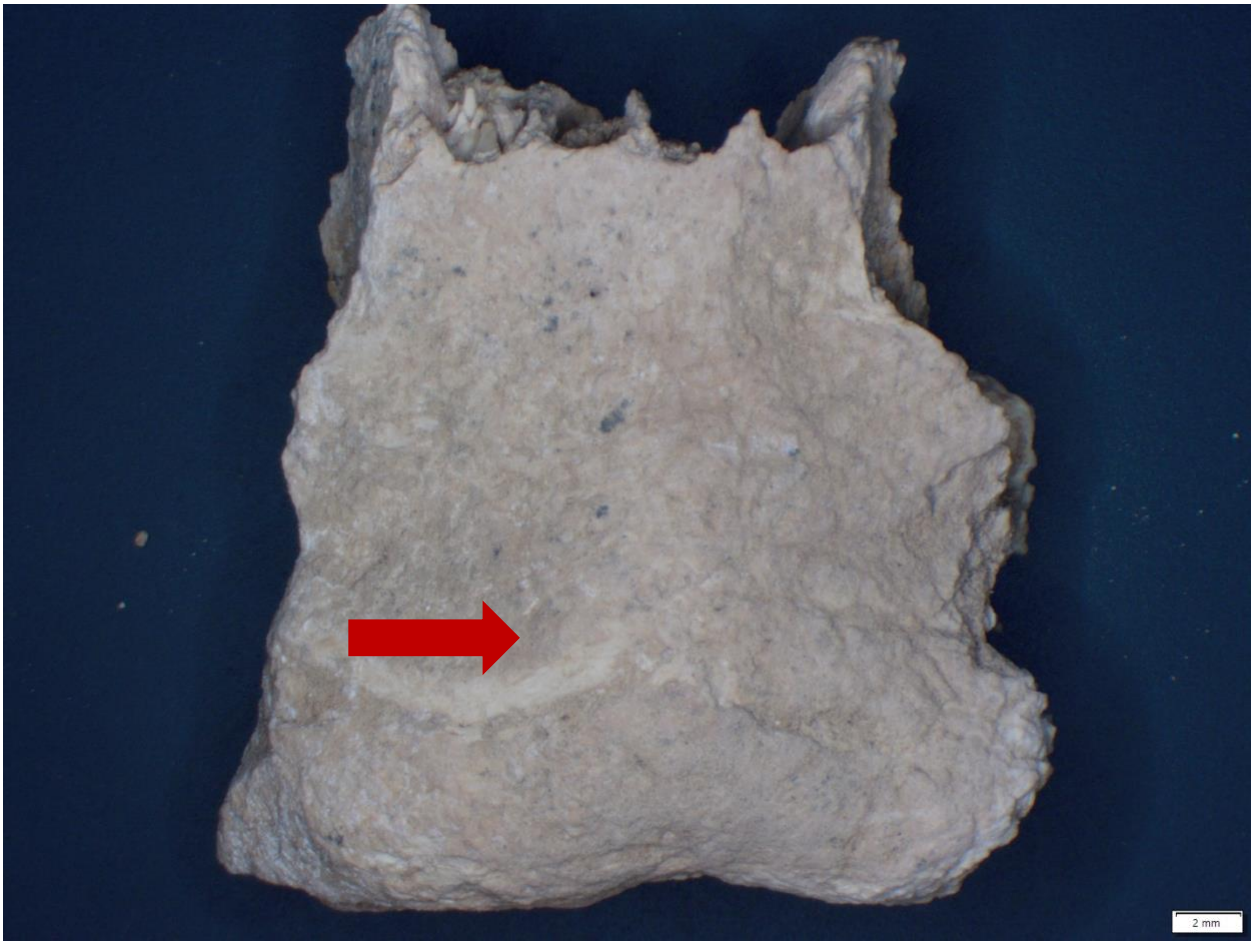

Figure A.4: Mental eminence, Locus 1- mandible, anterior, adult

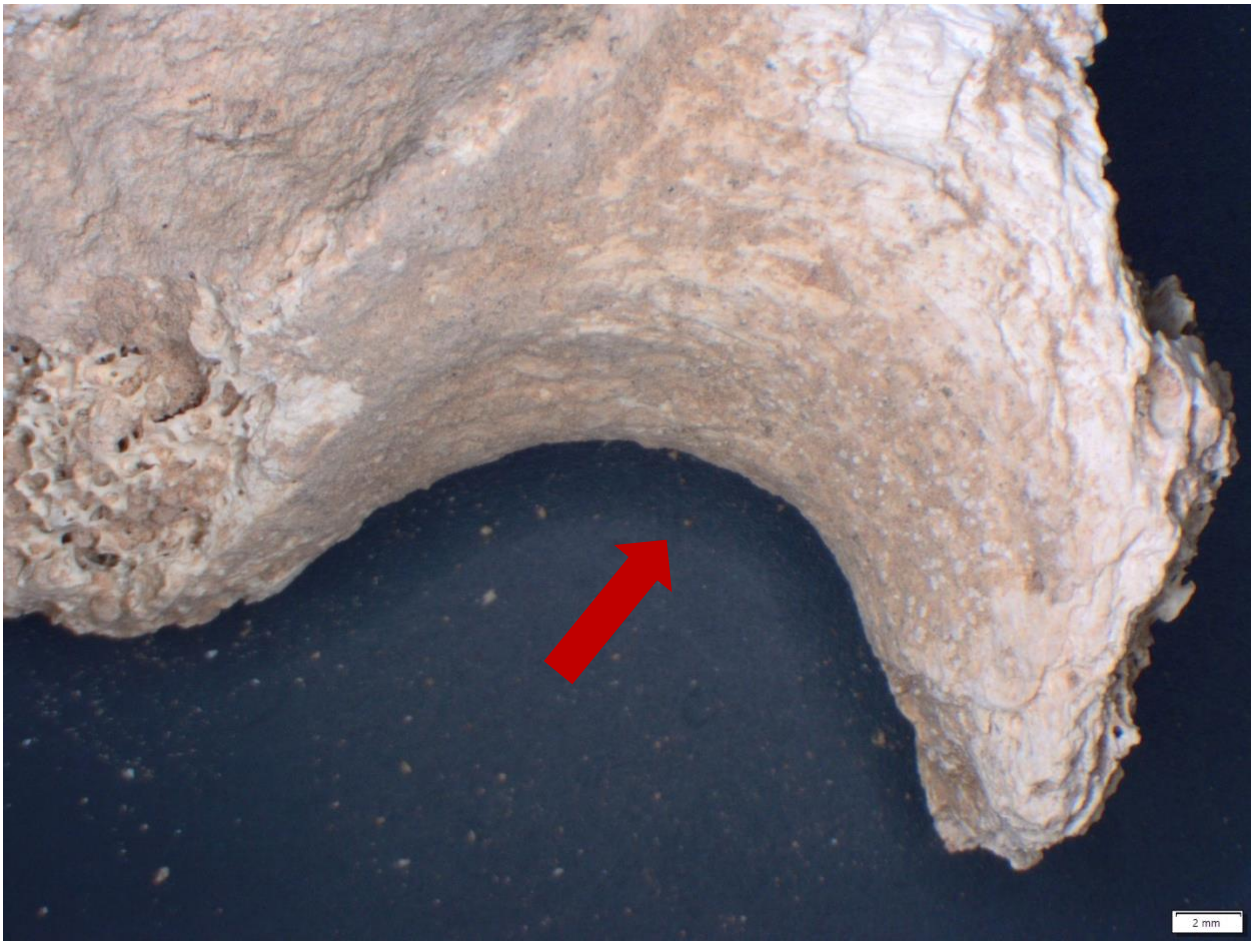

Figure A.5: Greater sciatic notch, Locus 4- left pelvis, medial, adult

Appendix B: Age-at-Death Estimation Indicators

B.1: Adult Age-at-Death Estimation Indicators

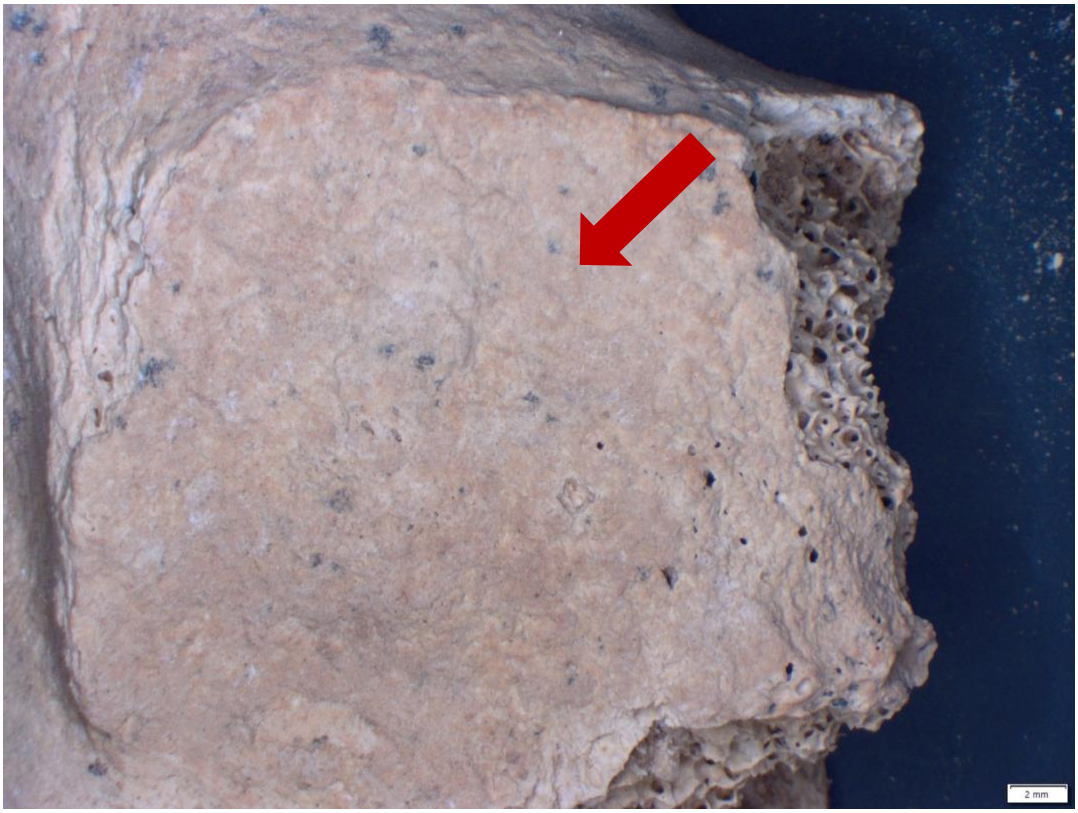

Figure B.1.6: Auricular surface, Locus 1- left pelvis, medial, adult

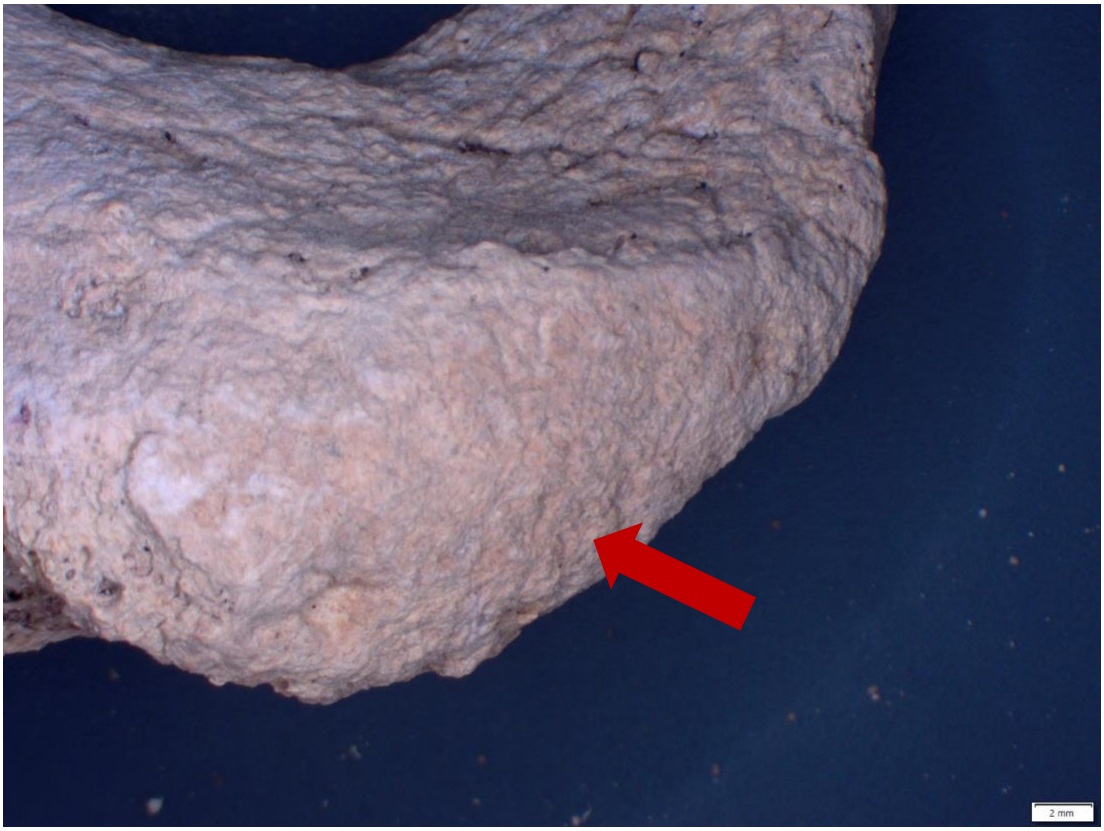

Figure B.1.7: Pubic symphysis, Locus 1- right pelvis, anterior, adult

Figure B.1.8: Auricular surface, Locus 4- left pelvis, medial, adult

B.2: Subadult Age-at-Death Indicators

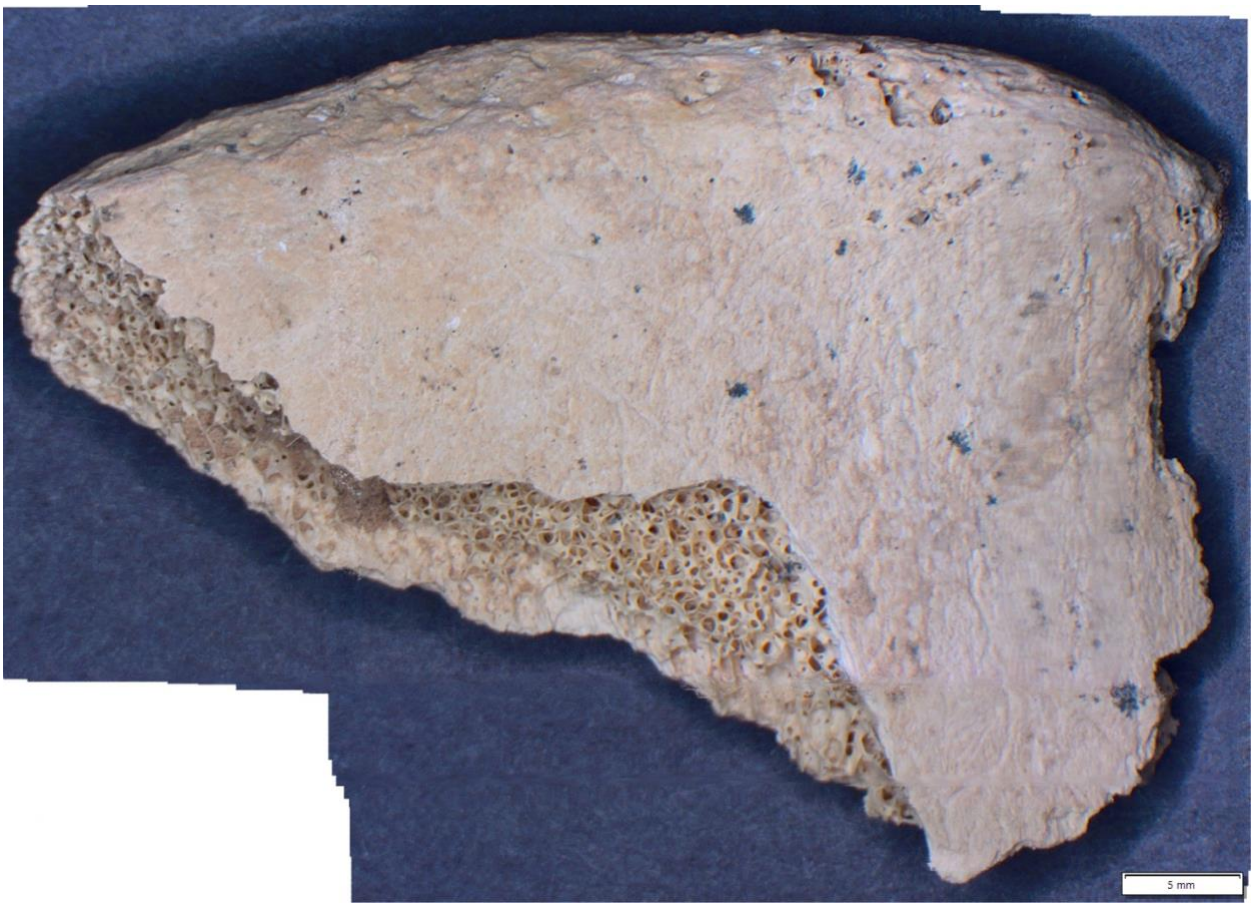

Figure B.2.9: Ilium, Locus 4- right pelvis, lateral, subadult

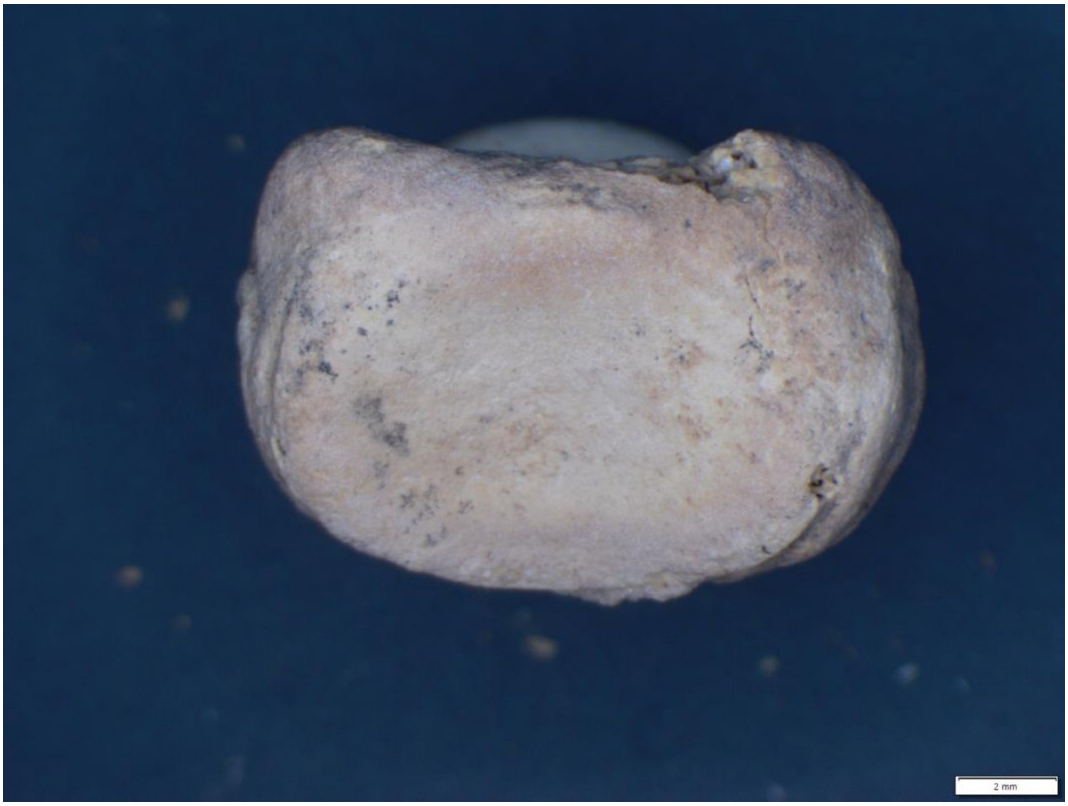

Figure B.2.10: Phalange, Locus 99- phalange, proximal surface, subadult

Figure B.2.11: Ischium, Locus 99- left pelvis, medial, subadult

Figure B.2.12: Femur head, Locus 99- anterior, subadult 8 years-old

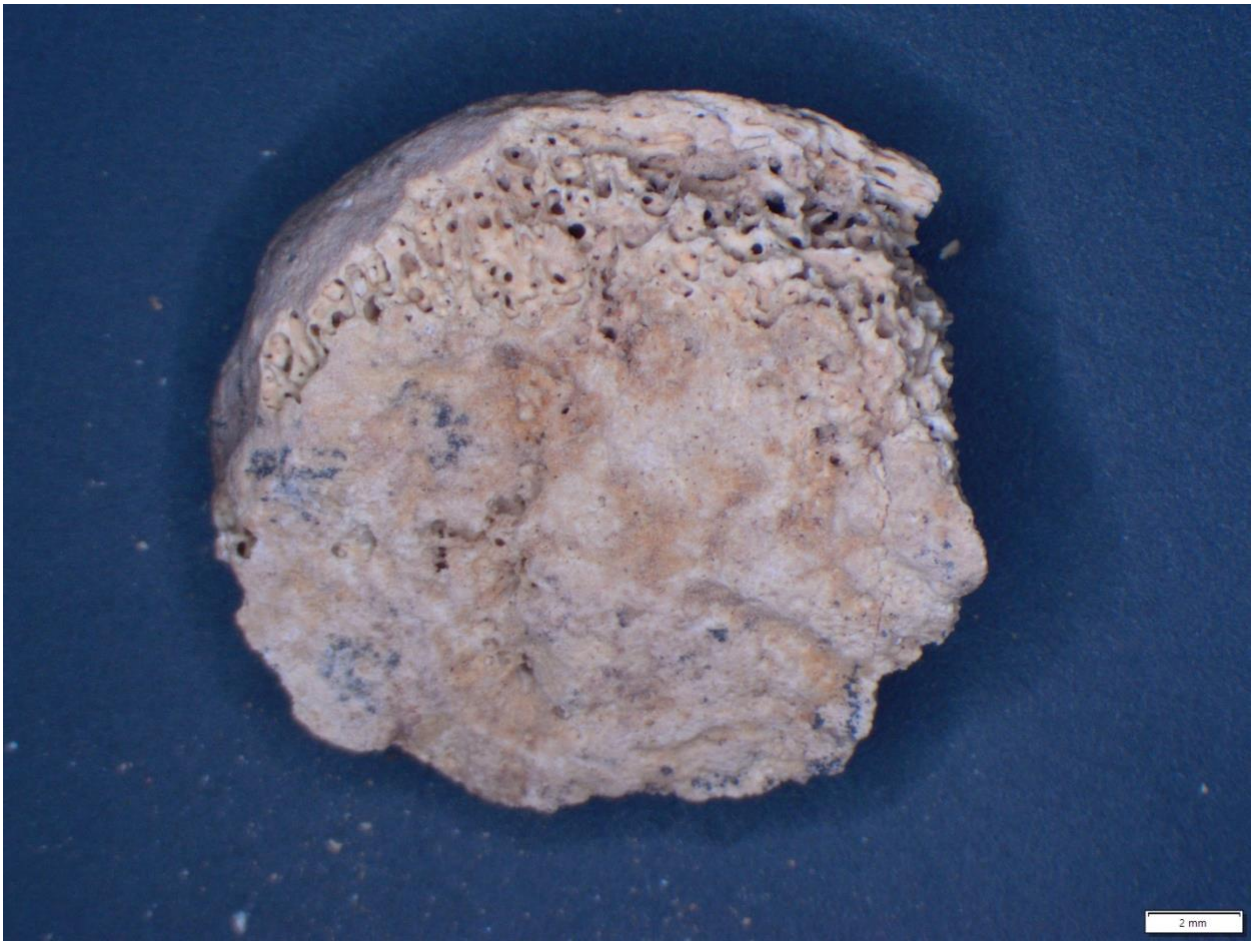

Figure B.2.13: Femur head, Locus 99- anterior, subadult 3 years-old

Figure B.2.14: Vertebrae, Locus 99- superior, subadult 6 years-old

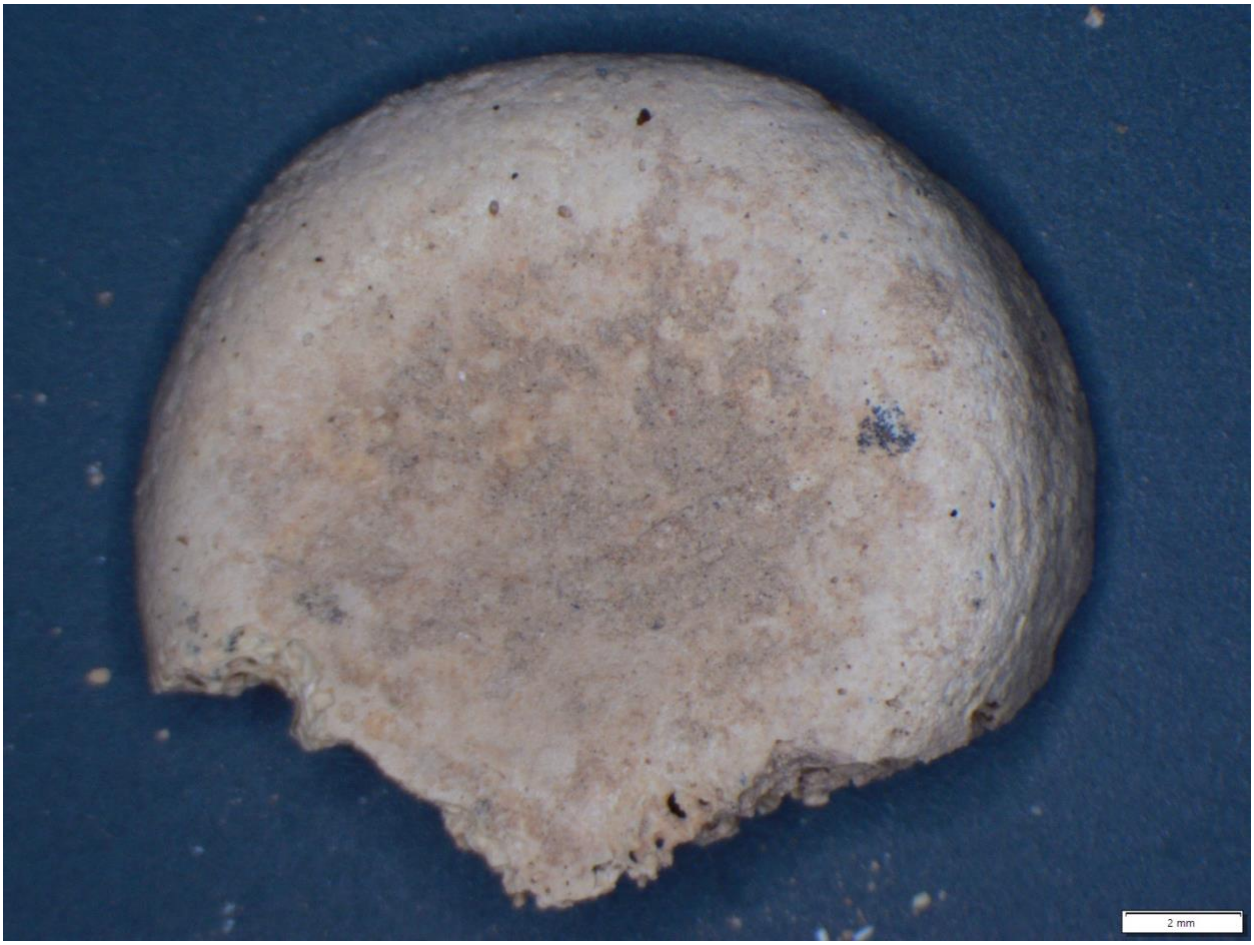

Figure B.2.15: Radius, Locus 99- proximal epiphysis, subadult

Appendix C: Pathology Indicators

Figure C.16: Bony growth, Locus 1- phalange, anterior, adult

Figure C.17: Bony growth, Locus 99- phalange, lateral, adult

Figure C.18: Enlarged Muscle Attachment, Locus 4- metacarpal, posterior, adult

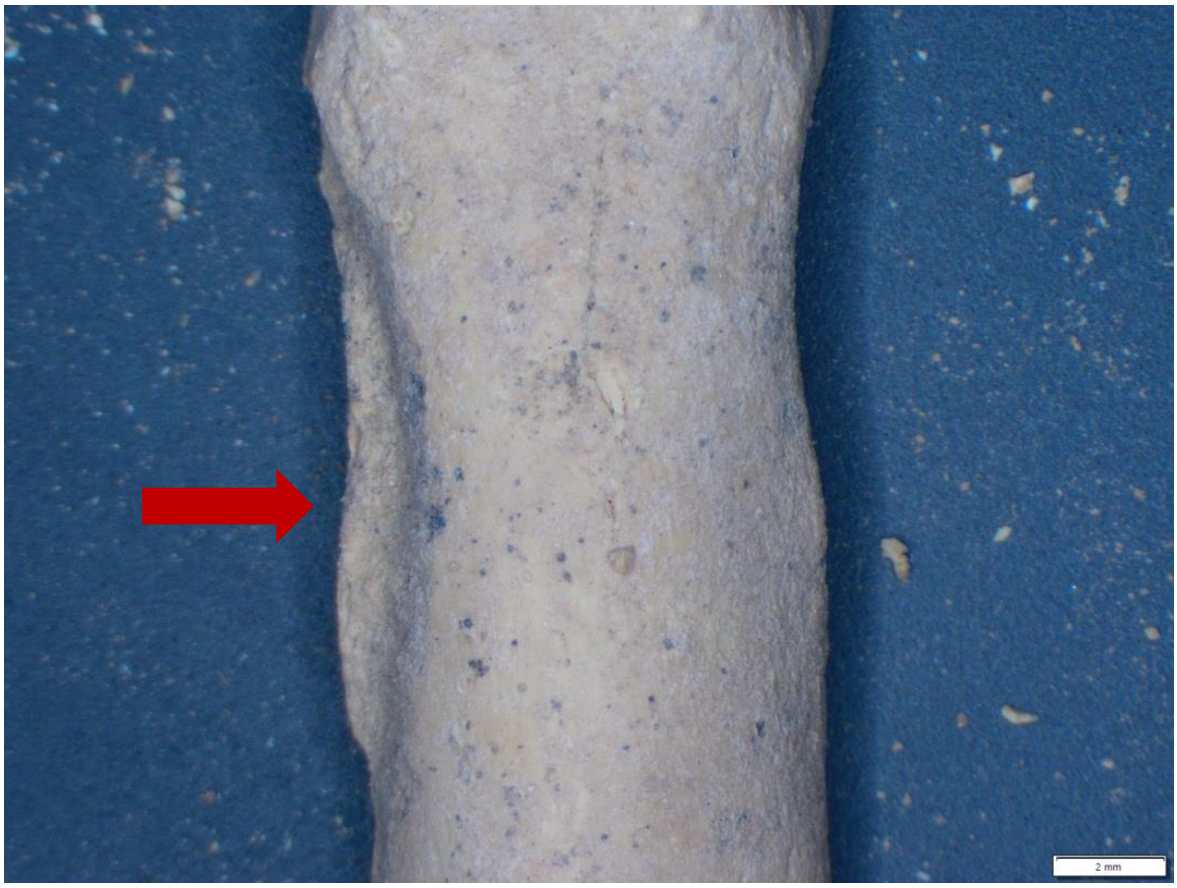

Figure C.19: Enlarged muscle attachment, Locus 99- proximal hand phalange, posterior, adult

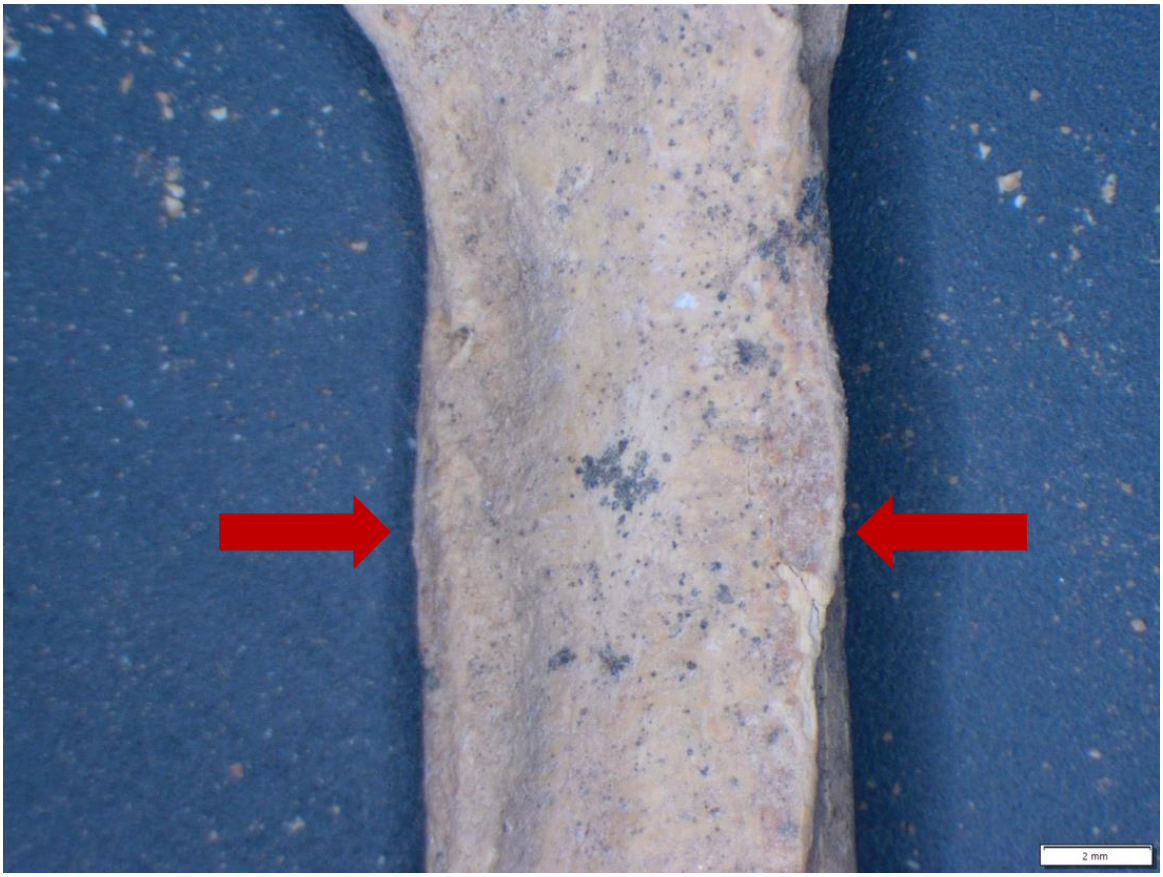

Figure C.20: Enlarged muscle attachment, Locus 99- proximal hand phalange, posterior, adult

Figure C.21: Striation markings, Locus 99- proximal foot phalange, posterior, adult

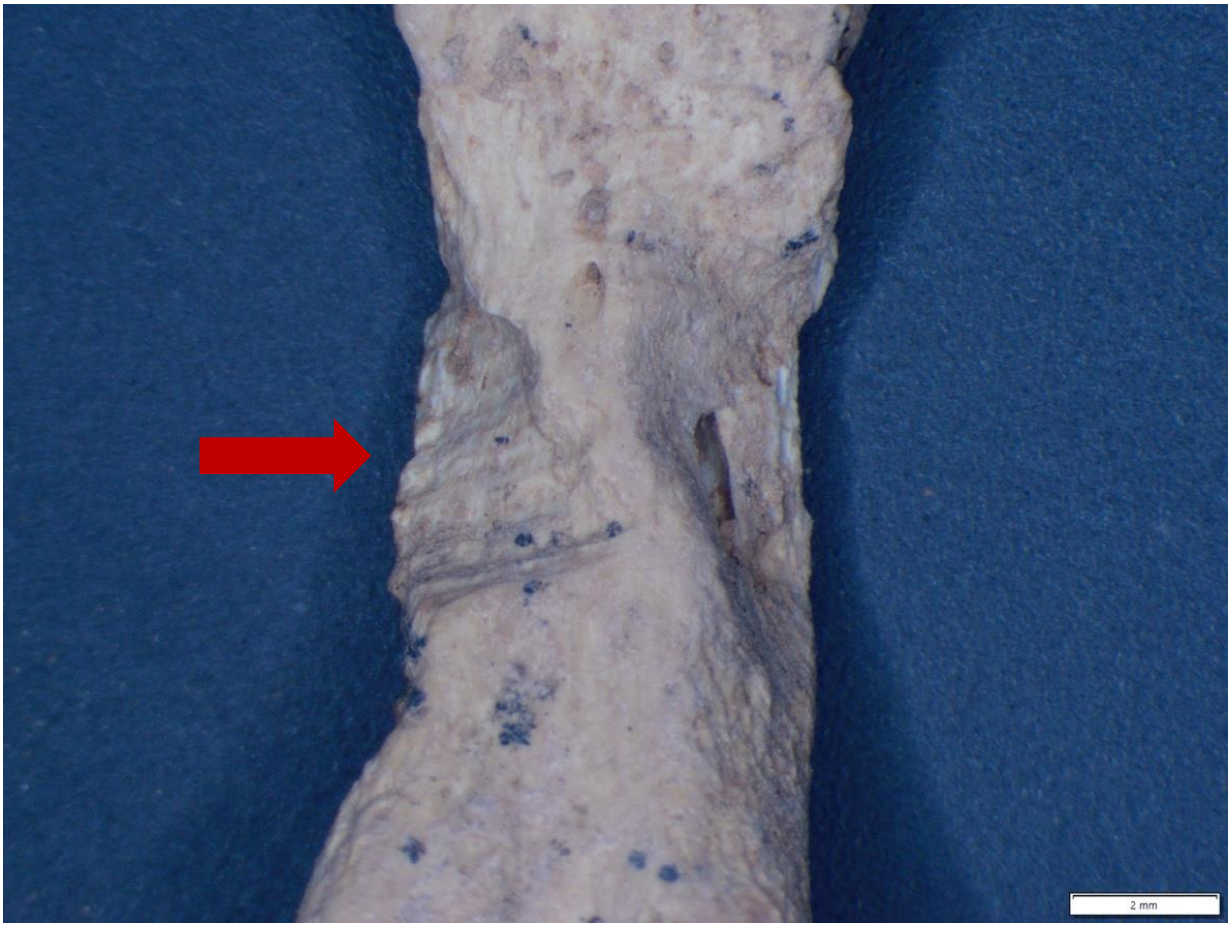

Figure C.22: Striation markings, Locus 99- proximal foot phalange, anterior, adult

Figure C.23: Enlarged muscle attachment, Locus 99- intermediate hand phalange, posterior, adult

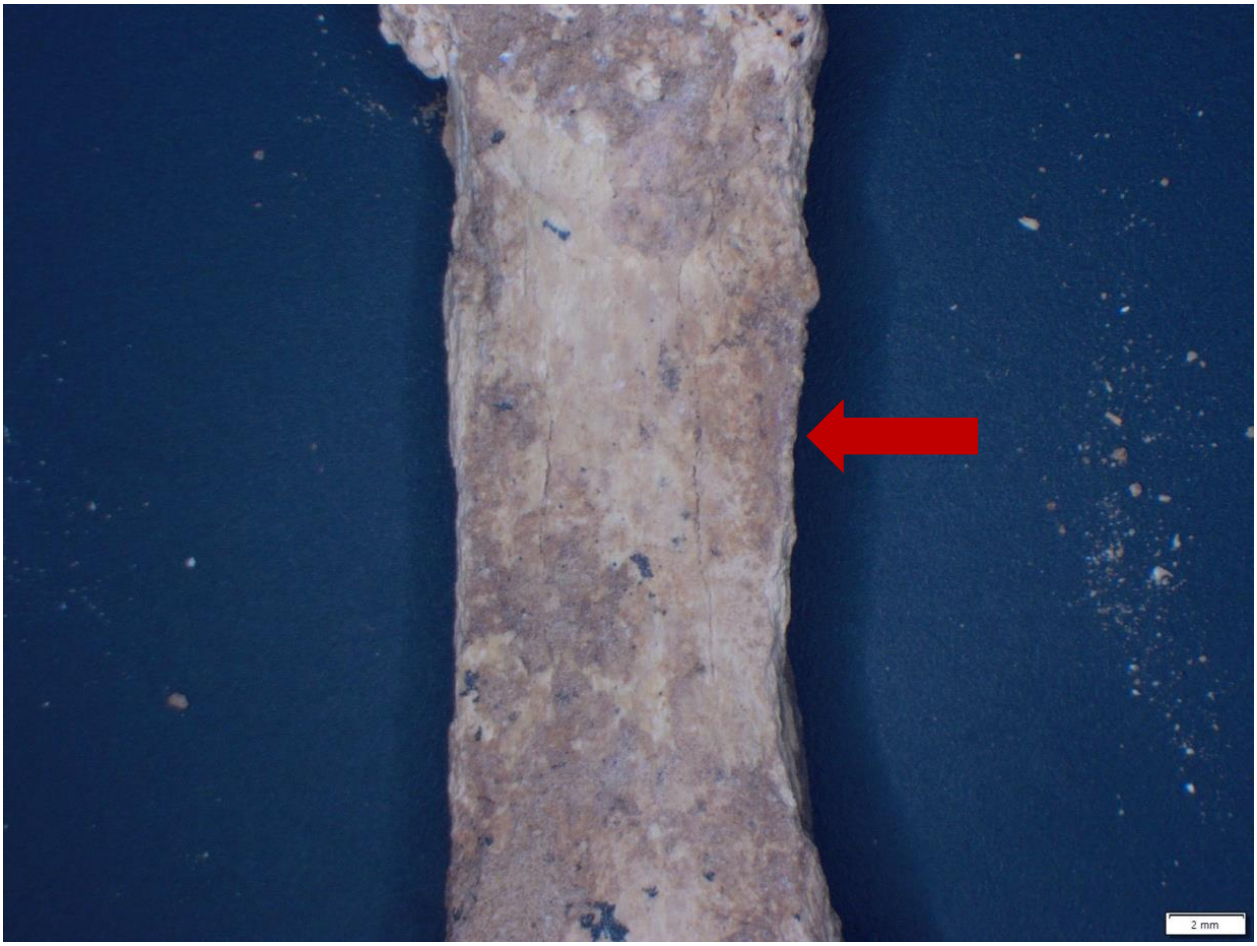

Figure C.24: Enlarged muscle attachment, Locus 99- intermediate hand phalange, anterior, adult

Figure C.25: Osteoarthritis, Locus 99- vertebrae body fragment, posterior, adult

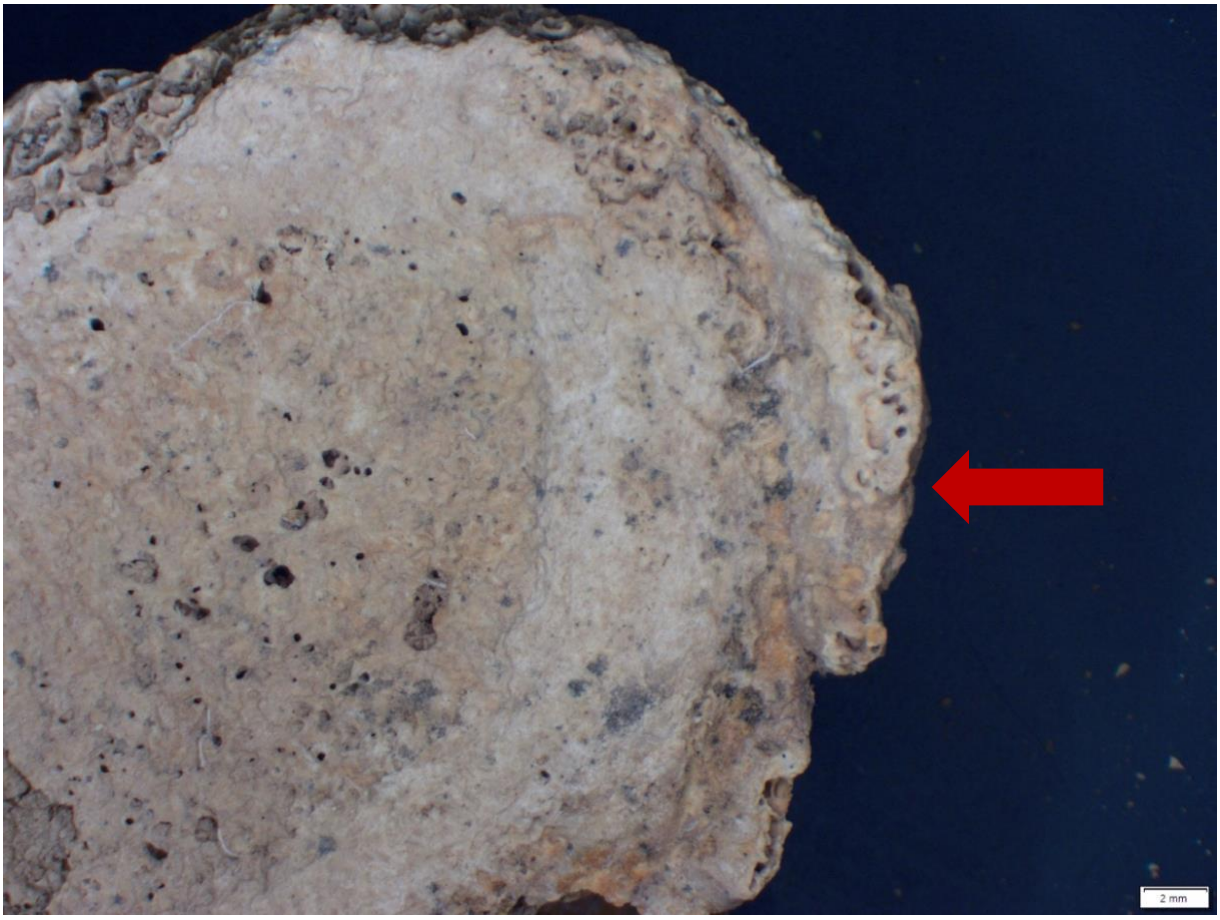

Figure C.26: Osteoarthritis, Locus 99- vertebrae body, superior, adult

Appendix D: Raw Inventory Data

Loot 3 Locus 1							
Box	**Bag**	**Bag/Box**	**Classifications of fragments**	**Measurement**	**Age**	**Notes**	**Sex**
Box 1	1 of 6		vertebrae head	28.82mm			
			mental protuberance of mandible	29.75mm			
			intermediate hand phalange	27.42mm			
			unidentified side metacarpal	28.35mm			
			long bone fragment	80.02mm			
			occipital bone	58.44mm			
			left metacarpal	42.38mm			
			right metatarsal head	16.09mm			
			zygomatic	24.50mm			
			zygomatic	35.03mm			
			right maxilla with *in situ* tooth	30.15mm	subadult		
Box 2	1 of 6		intermediate hand phalange	15.89mm			
			intermediate hand phalange	19.38mm			
			proximal hand phalange	35.33mm			
			unidentified phalange	26.14mm			
			intermediate foot phalange	19.00mm			
			distal hand phalange	17.96mm			
			phalange	17.60mm	subadult	rim on diaphysis; deep crevasses	
			intermediate hand phalange	21.48mm			
			proximal foot phalange	26.38mm		lipping and muscle lines on the side	
			unidentifiable side metatarsal proximal end fragment	32.46mm			
			unidentifiable side metatarsal	55.04mm			
			unidentifiable side metatarsal fragment	39.76mm			

Box	Bag	Bag/Box	Classifications of fragments	Measurement	Age	Notes	Sex
			rib fragment	33.39mm			
			skull fragment	35.01mm			
			skull fragment	31.03mm			
			skull fragment	59.31mm			
			skull fragment	39.85mm			
			skull fragment	37.05mm			
			skull fragment	32.38mm			
			skull fragment	35.31mm			
			skull fragment	54.61mm			
			skull fragment	72.40mm			
			skull fragment	35.07mm			
			superciliary arch; metopic suture; supraorbital notch; supraorbital margin	55.96mm	adult	metopic suture still visible- either a non metric trait or a subadult under the age of 8	male?
			vertebral arch fragment	19.74mm	has potential to be subadult		
			possible humerus head?	23.13mm	subadult	grooves at the top	
			distal end of ulna	49.08mm			
			long bone shaft fragment	73.42mm			
			long bone shaft fragment	37.51mm			
			long bone shaft fragment	33.47mm			
			long bone shaft fragment	57.64mm			
			long bone shaft fragment	62.17mm			
			long bone shaft fragment	71.25mm			
			ilium crest?	28.62mm		crest is visible	
			acetabular of the ilium	40.45mm	subadult		
			proximal hand phalange	11.09mm	subadult	concave auricular surface	
	1 of 4		right mandible fragment	41.99mm		right mental foramen helped side	
			mandible fragment	29.21mm			
			mandible fragment	18.29mm			

Box	Bag	Bag/Box	Classifications of fragments	Measurement	Age	Notes	Sex
			left mandible fragment	61.14mm			
			skull fragment	16.80mm			
			skull fragment	32.45mm			
			skull fragment	30.80mm			
			skull fragment	31.23mm			
			skull fragment	26.14mm			
			skull fragment	30.64mm			
			skull fragment	46.84mm			
			skull fragment	45.80mm		suture lines visible	
			skull fragment	39.01mm			
			skull fragment	45.16mm			
			skull fragment	27.79mm			
			skull fragment	33.50mm			
			skull fragment	26.39mm			
			skull fragment	23.37mm			
			skull fragment	74.63mm			
			long bone shaft fragment	43.54mm			
			long bone shaft fragment	33.58mm			
			long bone shaft fragment	39.66mm			
			long bone shaft fragment	27.80mm			
			long bone shaft fragment	34.91mm			
			long bone shaft fragment	48.93mm			
			long bone shaft fragment	67.45mm			
			long bone shaft fragment	53.15mm			
			long bone shaft fragment	43.50mm			
			intermediate foot phalange	27.25mm		boney growth on side of phalange	
			intermediate hand phalange	37.17mm			
			unidentifiable side metatarsal fragment	37.77mm			

Box	Bag	Bag/Box	Classifications of fragments	Measurement	Age	Notes	Sex
			unidentified metatarsal proximal end fragment	34.02mm			
			proximal epiphysis of humerus	20.76mm	subadult		
			proximal epiphysis of ulna	43.95mm	subadult		
			humerus proximal end fragment	41.18mm			
			unidentifiable side lunate	18.44mm			
			left capitate	18.48mm	possible subadult?		
	1 of 4		intermediate foot phalange	26.18mm			
			intermediate hand phalange	18.78mm			
			intermediate hand phalange	21.43mm			
			proximal foot phalange	28.90mm			
			intermediate foot phalange	16.62mm			
			skull fragment	42.08mm			
			skull fragment	28.67mm			
			skull fragment	51.68mm			
			skull fragment	21.89mm			
			skull fragment	21.14mm			
			skull fragment	23.60mm			
			skull fragment	33.26mm			
			skull fragment	32.45mm			
			skull fragment	28.15mm			
			skull fragment	53.78mm			
			skull fragment	41.01mm			
			skull fragment	30.72mm			
			skull fragment	27.46mm			
			right zygomatic bone	39.81mm			
			skull fragment	30.49mm			
			skull fragment	23.24mm			

Box	Bag	Bag/Box	Classifications of fragments	Measurement	Age	Notes	Sex
			skull fragment	14.54mm		suture lines	
			skull fragment	57.58mm			
			long bone shaft fragment	105.56mm			
			rib fragment	45.43mm			
			long bone shaft fragment	44.36mm			
			long bone shaft fragment	48.62mm			
			long bone shaft fragment	56.33mm			
			long bone shaft fragment	57.18mm			
			long bone shaft fragment	41.04mm			
			femur head fragment proximal end	50.02mm			
			proximal epiphysis of tibia	32.46mm	subadult		
			ulnar distal epiphysis fragment	29.65mm	subadult		
			ulnar proximal epiphysis fragment	48.84mm			
			fragment of pelvic girdle - greater sciatic notch & auricular surface	63.73mm	approx. 35-40 years old		possible female?
	1 of 6		right radius	90.04mm	adult	missing the proximal end	
			left radius	48.59mm	adult	proximal end fused	
			potentially a right radius	46.74mm	adult	proximal end fused	
			right ulna	43.78mm	subadult	not fused	
			long bone shaft fragment	96.67mm			
			long bone shaft fragment	49.72mm			
			long bone shaft fragment	71.59mm			
			long bone shaft fragment	42.57mm			
			long bone shaft fragment	60.51mm			
			long bone shaft fragment	50.29mm			
			long bone shaft fragment	56.65mm			
			long bone shaft fragment	36.16mm			

Box	Bag	Bag/Box	Classifications of fragments	Measurement	Age	Notes	Sex
			long bone shaft fragment	56.22mm			
			long bone shaft fragment	90.32mm			
			long bone shaft fragment	68.78mm			
			long bone shaft fragment	81.04mm			
			long bone shaft fragment	67.71mm		very clean break	
			long bone shaft fragment	47.39mm			
			long bone shaft fragment	38.84mm			
			long bone shaft fragment	59.09mm			
			long bone shaft fragment	40.44mm			
			long bone shaft fragment	39.04mm			
			long bone shaft fragment	48.22mm			
			long bone shaft fragment	49.58mm			
			long bone shaft fragment	48.06mm			
			long bone shaft fragment	39.27mm			
			rib shaft fragment	33mm			
			rib shaft fragment	28.41mm			
			rib shaft fragment	35.60mm			
			rib shaft fragment	30.01mm			
			right zygomatic bone	50.72mm			
			skull fragment	36.23mm		suture lines	
			skull fragment	32.61mm			
			skull fragment	44.08mm			
			skull fragment	33.99mm		suture lines	
			orbital bone fragment	36.65mm			
			left orbital bone fragment	44.07mm		supraorbital notch	
			skull fragment	37.01mm		suture lines	
			skull fragment	43.86mm			
			skull fragment	53.31mm			
			skull fragment	36.01mm			

Box	Bag	Bag/Box	Classifications of fragments	Measurement	Age	Notes	Sex
			skull fragment	26.78mm			
			skull fragment	28.77mm			
			frontal bone fragment	56.99mm			
			right parietal bone	62.13mm			
			skull fragment	24.43mm			
			skull fragment	33.98mm			
			humerus distal end	42.10mm			
			femur head fragment	28.50mm			
			tibia proximal epiphysis	49.57mm			
			tibia proximal epiphysis fragment	33.85mm			
			acetabulum fragment	49.58mm		right	
			unidentified side metatarsal	63.05mm			
			proximal hand phalange	36.13mm			
			intermediate hand phalange	18.07mm			
			unidentified side metatarsal proximal end	30.88mm			
			unidentified side metatarsal proximal end	43.72mm			
			unidentified side metatarsal distal end fragment	30.26mm			
			vertebrae fragment	30.54mm			
			vertebrae arch fragment	31.67mm			
			vertebrae fragment	21.98mm			
			vertebrae fragment	25.47mm			
			vertebrae fragment	22.21mm			
			vertebrae fragment	21.67mm			
			vertebrae fragment	33.16mm			
			vertebrae fragment	26.73mm			
			vertebrae fragment	25.28mm			
			vertebrae body fragment	18.92mm	subadult	no border on body	

Box	Bag	Bag/Box	Classifications of fragments	Measurement	Age	Notes	Sex
			vertebrae body fragment	37.85mm	subadult	no border on body	
	1 of 5		long bone shaft fragment	48.34mm			
			long bone shaft fragment	50.38mm			
			long bone shaft fragment	31.30mm			
			long bone shaft fragment	66.19mm			
			long bone shaft fragment	55.57mm			
			long bone shaft fragment	26.04mm			
			long bone shaft fragment	68.06mm			
			long bone shaft fragment	30.32mm			
			long bone shaft fragment	61.12mm			
			long bone shaft fragment	58.90mm			
			long bone shaft fragment	54.34mm			
			rib shaft fragment	34.17mm			
			intermediate foot phalange	24.01mm			
			proximal foot phalange	26.69mm			
			intermediate hand phalange	24.69mm			
			skull fragment	30.90mm		suture lines	
			skull fragment	33.63mm		suture lines	
			skull fragment	30.46mm			
			skull fragment	38.54mm			
			skull fragment	47.57mm			
			skull fragment	37.20mm			
			skull fragment	24.78mm		possible zygomatic	
			skull fragment	39.23mm			
			skull fragment	32.65mm			
			skull fragment	57.81mm			
			parietal fragment	70.99mm		suture lines	
			occipital bone	71.58mm		suture lines	
			skull fragment	32.09mm			

Box	Bag	Bag/Box	Classifications of fragments	Measurement	Age	Notes	Sex
			skull fragment	45.37mm			
			skull fragment	23.03mm			
			skull fragment	39.21mm			
			skull fragment	28.93mm			
			skull fragment	57.86mm			
			parietal fragment	55.96mm			
			skull fragment	46.27mm			
			skull fragment	56.30mm		suture lines	
			left parietal bone	56.33mm			
			skull fragment	66.03mm			
			skull fragment	32.14mm			
			skull fragment	47.88mm			
			skull fragment	63.89mm			
			skull fragment	43.81mm			
			skull fragment	42.05mm		suture lines- suture ossicle present	
			skull fragment	31.94mm			
			skull fragment	29.69mm	minimal suture closure- young adult	suture lines visible	
			humeral proximal end	37.99mm	subadult	pitted head- possible subadult	
			acromion process	58.06mm		of right scapula	
			right ulnar head	36.97mm	adult?		
			right (?) clavicle	74.95mm			
			left (?) clavicle	53.93mm			
			vertebrae body fragment	32.02mm	subadult		
			vertebrae fragment	27.19mm			
			vertebrae fragment	32.72mm			
			vertebrae fragment	31.92mm			
			vertebrae fragment	18.70mm			
			pars basilaris of occipital bone	42.57mm	adult?	sides are very curved and defined	

Box	Bag	Bag/Box	Classifications of fragments	Measurement	Age	Notes	Sex
	1 of 4		skull fragment	25.34mm			
			skull fragment	39.58mm			
			skull fragment	32.91mm			
			skull fragment	41.05mm			
			skull fragment	22.58mm			
			skull fragment	39.65mm		suture lines	
			skull fragment	26.55mm			
			skull fragment	29.54mm			
			skull fragment	36.31mm			
			skull fragment	37.02mm			
			skull fragment	48.05mm			
			skull fragment	25.49mm			
			skull fragment	30.61mm			
			skull fragment	18.46mm		suture lines	
			skull fragment	20.46mm			
			skull fragment	35.14mm			
			skull fragment	26.17mm			
			skull fragment	39.47mm			
			skull fragment	31.73mm			
			skull fragment	31.98mm			
			skull fragment	29.77mm			
			skull fragment	27.90mm			
			skull fragment	23.89mm			
			skull fragment	24.95mm			
			skull fragment	30.34mm		suture lines	
			skull fragment	20.71mm		suture lines	
			skull fragment	28.85mm			
			skull fragment	26.24mm			
			skull fragment	16.56mm		suture lines	

Box	Bag	Bag/Box	Classifications of fragments	Measurement	Age	Notes	Sex
			skull fragment	24.54mm			
			skull fragment	23.58mm			
			rib shaft fragment	34.64mm			
			rib shaft fragment	21.04mm			
			rib shaft fragment	25.50mm			
			rib shaft fragment	35.87mm			
			rib fragment- right 1st rib	50.40mm			
			rib shaft fragment	24.96mm			
			rib shaft fragment	29.62mm			
			rib shaft fragment	38.11mm			
			rib shaft fragment	35.62mm			
			rib shaft fragment	24.13mm			
			rib shaft fragment	41.35mm			
			rib shaft fragment	22.78mm			
			long bone shaft fragment	38.80mm			
			long bone shaft fragment	43.06mm		straight edge cut	
			long bone shaft fragment	50.43mm			
			long bone shaft fragment	82.30mm			
			long bone shaft fragment	83.66mm			
			long bone shaft fragment	81.36mm			
			long bone shaft fragment	52.35mm			
			long bone shaft fragment	89.04mm			
			long bone shaft fragment	40.22mm			
			long bone shaft fragment	51.35mm			
			long bone shaft fragment	67.31mm			
			long bone shaft fragment	54.56mm			
			long bone shaft fragment	129.80mm			
			unidentified side metatarsal proximal end fragment	39.91mm			
			phalange fragment	27.92mm			

Box	Bag	Bag/Box	Classifications of fragments	Measurement	Age	Notes	Sex
			proximal foot phalange	29.16mm			
			unidentified side metatarsal	41.46mm			
			proximal hand phalange shaft fragment	31.85mm		boney growth	
			proximal hand phalange	28.14mm			
			unidentified side metacarpal	37.62mm			
			proximal hand phalange	14.68mm			
			proximal hand phalange	32.39mm			
			distal 1 hand phalange	18.35mm			
			phalange shaft fragment	28.08mm			
			intermediate hand phalange	16.81mm			
			intermediate hand phalange	15.54mm			
			distal hand phalange	10.03mm			
			proximal hand phalange	15.77mm	subadult		
			proximal hand phalange	15.57mm	subadult		
			phalange shaft fragment	12.42mm	subadult		
			proximal hand phalange	16.37mm	subadult		
			intermediate hand phalange	12.33mm	subadult		
			vertebrae body fragment	21.93mm	subadult	grooved body	
			vertebrae body fragment	26.70mm	adult?	defined border	
			vertebrae body fragment	36.71mm	adult	defined border	
			vertebrae arch fragment	27.62mm			
			vertebrae body fragment	25.49mm			
			spinous process fragment	22.78mm			
			vertebrae body fragment	22.26mm	adult	signs of osteoarthritis	
			vertebrae body	42.14mm	adult		
			femur head fragment	33.80mm			
			distal condyle of femur	37.27mm			
			radial proximal epiphysis	16.70mm	subadult	fovea	

Box	Bag	Bag/Box	Classifications of fragments	Measurement	Age	Notes	Sex
			medial epicondyle of distal end of humerus	26.12mm			
			humerus or femur head	24.86mm			
			unidentifiable side lunate	18.28mm			
			right hamate	16.67mm			
			left hamate	20.15mm			
			distal epiphysis of humerus	18.42mm	subadult		
			distal epiphysis of humerus	14.88mm	subadult		
			proximal end of femur	61.12mm	subadult		
Box 3	in box		right pelvis		adult- 22-26 years old	pubic symphysis- 2/3 on todd and 2/3 on suchey-brooks-- no defined border around	female
			left pelvis			more fragmented	
	1 of 6		left side of mandible fragment	50.44mm	adult		
			proximal hand phalange	32.76mm			
			distal hand phalange	19.91mm			
			rib shaft fragment	27.45mm			
			rib shaft fragment	30.41mm			
			rib shaft fragment	28.85mm			
			rib shaft fragment	27.53mm			
			long bone shaft fragment	108.29mm			
			long bone shaft fragment	43.22mm			
			long bone shaft fragment	69.79mm			
			long bone shaft fragment	57.39mm			
			long bone shaft fragment	60.30mm			
			long bone shaft fragment	49.38mm			
			long bone shaft fragment	47.97mm			
			vertebrae body fragment	38.43mm			
			vertebrae fragment	29.87mm			
			skull fragment	20.80mm		suture lines	

Box	Bag	Bag/Box	Classifications of fragments	Measurement	Age	Notes	Sex
			frontal bone fragment	31.55mm		suture lines	
			skull fragment	40.00mm		suture lines	
			skull fragment	31.06mm		suture lines	
			skull fragment	38.90mm			
			skull fragment	27.50mm			
			skull fragment	49.01mm			
	2 of 5		right patella	29.20mm			
			vertebrae body fragment	22.93mm			
			skull fragment	35.67mm	subadult	suture lines-pretty open	
			skull fragment	30.93mm			
			skull fragment	23.75mm			
			skull fragment	30.03mm			
			skull fragment	40.95mm			
	1 of 10		mandible fragment	34.71mm			
			left mandible fragment	71.77mm		adult mandible- no room for baby teeth	
			mandible fragment - teeth holes	28.32mm			
			mandible fragment - teeth holes	28.26mm			
			humeral head	38.97mm	adult	no fossa like in femur head	
			left humeral distal end	58.51mm	adult	fused together	
			vertebrae body fragment	27.00mm	adult		
			acromion process of scapula	52.02mm			
			rib shaft fragment	29.12mm			
			rib shaft fragment	34.67mm			
			rib shaft fragment	51.65mm			
			rib shaft fragment	44.48mm			
			spinous process fragment	24.17mm			
			radial shaft fragment	52.77mm		radial tuberosity	

Box	Bag	Bag/Box	Classifications of fragments	Measurement	Age	Notes	Sex
			unidentifiable side metatarsal 1 fragment	34.43mm			
			unidentifiable side metatarsal fragment	40.86mm			
			skull fragment	40.95mm		suture lines- pretty open sutures	
			skull fragment	35.38mm		suture lines- pretty open sutures	
			skull fragment	40.61mm			
			skull fragment	26.34mm		suture lines- pretty open sutures	
			skull fragment	50.60mm	adult	c- significant closure on suture lines	
			skull fragment	51.50mm	adult	c- significant closure on suture lines	
			right parietal bone	92.06mm			
	1 of 5		radial head fragment	19.78mm	adult		
			tibial epiphysis end fragment	22.18mm	subadult	unfused	
			capitulum and trochlea end of humerus fragment	24.77mm		cannot determine whether its adult or subadult	
			right navicular fragment	31.05mm	subadult	smaller than typical adult	
			proximal end of hand phalange	35.73mm			
			intermediate hand phalange	22.59mm			
			rib fragment- 1st rib	36.44mm		possible subadult	
			rib shaft fragment	25.81mm			
			skull fragment	23.99mm		suture lines- open lines	
			skull fragment	28.79mm		suture lines- open lines	
			skull fragment	57.68mm		suture lines- significant closure	
			skull fragment	45.28mm		suture lines- significant closure	
			skull fragment	36.30mm		suture lines- closed	
			skull fragment	39.10mm		suture lines- minimal closure	
			skull fragment	30.23mm		suture lines- significant closure	
			mandible fragment	40.70mm			
			orbital bone fragment	25.09mm			
			radial bone shaft fragment	95.14mm			

Box	Bag	Bag/Box	Classifications of fragments	Measurement	Age	Notes	Sex
	no bag #		vertebrae body fragment	22.44mm	subadult		
			rib shaft fragment	36.28mm			
			rib shaft fragment	30.22mm			
			rib shaft fragment	24.85mm			
			intermediate hand phalange	24.66mm			
			distal hand phalange	19.57mm	possible subadult?		
			proximal hand phalange	26.52mm			
			unidentifiable side capitate fragment	19.90mm			
			unidentifiable side trapezoid	18.31mm			
			skull fragment	38.82mm		either frontal or occipital has a sagittal line	
			zygomatic fragment	32.56mm			
			skull fragment	27.58mm		minimal closure	
			zygomatic fragment	29.85mm			
			skull fragment	39.62mm		complete suture obliteration	
			skull fragment	38.44mm		significant suture closure	
			skull fragment	48.32mm		significant suture closure	
			post sphenoid fragment	27.55mm	infant		

Table D.1: Raw data for Locus 1

Loot 3 Locus 2							
Box	**Bag**	**Bag/Box**	**Classifications of fragments**	**Measurement**	**Age**	**Notes**	**Sex**
2	1 of 5		phalange	18.47mm			
			distal phalange	9.95mm			
			Unidentified side trapezoid carpal	12.83mm			
			Unidentified side trapezium carpal	24.41mm			
			skull fragment	39.40mm			
	5 of 5		right talus	36.51mm			
			Unidentified side navicular	22.94mm			
			Unidentified side calcaneus	37.77mm			
			proximal foot phalange	27.79mm			
			intermediate foot phalange	27.54mm			
			intermediate foot phalange	27.58mm			
			intermediate foot phalange	22.05mm			
			distal foot phalange	14.88mm			
			intermediate foot phalange	16.07mm			
			proximal foot phalange	56.20mm			
			Unidentified side calcaneus	22.93mm			
			Unidentified side cuboid	17.06mm			
			Unidentified side cuneiform	19.27mm			
			Unidentified side cuboid	33.54mm			

Table D.2: Raw data for Locus 2

Loot 3 Locus 3

Box	Bag	Bag/Box	Classifications of fragments	Measurement	Age	Notes	Sex
1	in box	8	right mandible	63.96mm	subadult	tooth still attached inside	
3	3 of 4	in box	long bone shaft fragments in tissue paper				
			long bone	78.80mm		I think its faunal - 2 puncture holes	
			right patella	37.71mm	adult		
			body of sternum	75.04mm		costal notches	
			unidentifiable side metacarpal	36.43mm	adult		
			intermediate hand phalange	22.23mm			
			intermediate hand phalange	27.37mm			
	1 of 4	in box	rib shaft fragment	51.60mm			
			intermediate foot phalange	10.12mm			
			intermediate foot phalange	10.83mm			
			proximal foot phalange	27.20mm			
			proximal foot phalange	30.56mm			
			unidentifiable side metatarsal distal end fragment	22.38mm			
			unidentifiable side metatarsal distal end fragment	31.77mm			
			unidentifiable side metatarsal proximal end fragment	48.05mm			
			intermediate foot phalange	11.86mm			
	1 of 4	in the tissue paper	long bone shaft fragment	89.28mm			
			long bone shaft fragment	48.99mm			
			radius long bone fragment	48.71mm			
			long bone shaft fragment	63.04mm			
			long bone shaft fragment	44.61mm			

Box	Bag	Bag/Box	Classifications of fragments	Measurement	Age	Notes	Sex
		in bag	skull fragment	39.48mm		suture lines	
			skull fragment	33.22mm		suture lines	
			skull fragment	33.32mm		suture lines	
			rib shaft fragment	48.99mm		possible floating rib- possible right	
			rib shaft fragment	63.39mm		Can't side- no ends	
			rib shaft fragment	36.81mm			
			rib shaft fragment	28.98mm			
			rib shaft fragment	28.18mm			
			rib shaft fragment	44.47mm			
			rib shaft fragment	31.55mm			
			rib shaft fragment	44.32mm			
			tibia head fragment	17.86mm	subadult		
			unidentifiable side metacarpal proximal end fragment	33.14mm			
			unidentifiable side metacarpal proximal end fragment	42.29mm			
			vertebrae body fragment	26.66mm	adult		
			unidentifiable side lunate carpal	17.37mm	possible subadult?	smaller than a regular sized lunate	
			unidentifiable side metatarsal fragment	33.78mm			
			distal hand phalange	10.69mm	subadult?	very tiny	
			distal hand phalange	16.88mm			
			intermediate foot phalange	11.73mm			
	1 of 1	SW corner	skull fragment	39.51mm		suture lines	
			skull fragment	30.93mm			
			skull fragment	25.30mm			
			rib shaft fragment	35.46mm			
			rib shaft fragment	54.60mm			
			right rib fragment	85.87mm			
			rib shaft fragment	132.69mm			

Box	Bag	Bag/Box	Classifications of fragments	Measurement	Age	Notes	Sex
			vertebrae fragment	36.84mm			
	1 of 4		proximal foot phalange	23.79mm			

Table D.3: Raw data for Locus 3

Loot 3 Locus 4

Box	Bag	Bag/Box	Classifications of fragments	Measurement	Age	Notes	Sex
2		In box- tissue paper	right femur shaft	15.7cm			
		In box- tissue paper	right humerus	19cm		distal end and shaft	
	1 of 7		intermediate hand phalange	25.71mm			
			intermediate foot phalange - big toe	32.58mm			
			intermediate hand phalange	20.71mm			
			thumb metacarpal - left (?)	41mm		lipping	
			distal hand phalange	18.46mm			
			intermediate hand phalange	23.55mm			
			left metatarsal 5	54.19mm			
			distal hand phalange	14.22mm			
			intermediate hand phalange	19.26mm			
			phalange fragment	20.91mm			
			right metatarsal head fragment	24.61mm			
			unidentifiable side metatarsal head fragment	13.32mm			
			unidentifiable side metatarsal head fragment	18.24mm			
			unidentifiable side metatarsal proximal end fragment	42.80mm			
			intermediate 1st foot phalange	32.14mm			
			right capitate	21.34mm			
			right lunate	14.55mm	subadult?		
			vertebrae body	37.73mm	adult	lumbar?	
			vertebrae body fragment	23.25mm	adult		
			vertebrae body	16.18mm	subadult?		
			vertebral arch	37.57mm			
			skull fragment	34.44mm			
			skull fragment	35.50mm			

Box	Bag	Bag/Box	Classifications of fragments	Measurement	Age	Notes	Sex
			skull fragment	24.51mm			
			skull fragment	33mm		slight signs of suture lines	
			skull fragment	29.47mm		suture lines	
			rib fragment	28.54mm			
			rib fragment	26.42mm			
			left rib fragment	39.90mm			
			rib fragment	32.13mm			
			rib fragment	30.70mm			
			left rib fragment	47.84mm			
			right rib fragment	57.32mm			
			rib fragment	45.80mm			
			rib fragment	32.09mm			
			ilium	58.10mm	subadult	between 2-5 years old- Molleson and Cox	
			glenoid cavity and supraglenoid tubercle of the left scapula	46.79mm	adult	coracoid process in tact	
			radial proximal end	39.21mm	subadult		
			distal end of humerus- capitulum	18.08mm			
			distal end of humerus- one of the condyles	18.52mm			
			ulna proximal end	39.19mm			
	3 of 7		distal phalange fragment	11.67mm	subadult		
	1 of 3		skull fragment	53.75mm			
			mandible fragment	54.54mm			
			mandible fragment	30.51mm			
			distal end of femur	41.82mm			
			femur head proximal end	47.11mm			
			femur head fragment proximal end	47.77mm			
			long bone shaft fragment	79.24mm			
			long bone shaft fragment	41.95mm			

Box	Bag	Bag/Box	Classifications of fragments	Measurement	Age	Notes	Sex
			long bone shaft fragment	46.11mm			
			long bone shaft fragment	70.38mm			
			proximal foot phalange	25.20mm			
			intermediate hand phalange	23.39mm		lipping on sides	
			intermediate hand phalange	19.03mm			
			unidentifiable side metatarsal foot fragment 1	28.40mm			
3	1 of 3		left scaphoid	24.68mm	subadult?	smaller than normal	
			distal epiphysis of tibia	16.70mm	subadult		
			proximal end of fibula?	29.17mm	subadult		
	1 of 3		left lunate	15.19mm			
			left capitate	22.32mm			
			intermediate hand phalange	14.43mm			
			distal hand phalange	24.71mm			
			distal foot phalange	10.46mm			
			proximal end of the proximal thumb phalange	24.41mm			
			rib shaft fragment	35.57mm			
	1 of 7	in tissue paper	left ulna	12.8cm	adult	fused together	
			vertebrae body fragment	27.97mm	subadult		
			proximal hand phalange	40.44mm			
			left capitate	21.10mm			
			skull fragment	32.61mm		minimal closure	
			rib shaft fragment	46.51mm			
			rib shaft fragment	38.92mm			
			rib shaft fragment	21.27mm			
			left pubic bone fragment	49.77mm	36-38 years	greater sciatic notch, auricular surface	male?

Table D.4: Raw data for Locus 4

Loot 3 Locus 5							
Box	**Bag**	**Bag/Box**	**Classifications of fragments**	**Measurement**	**Age**	**Notes**	**Sex**
1	1 of 5	skull bone tissue paper	right parietal	80.24mm		goes with the curve of the head	
			occipital	52.43mm		more flat; occipital sulcus	
			left rib	58.28mm			
			clavicle	75.42mm		too curved to be a long bone	
2	2 of 5		intermediate hand phalange 1	32.53mm			
3	1 of 1	in the box	radial shaft fragment	119.62mm	adult		
			left clavicle	89.64mm	adult		

Table D.5: Raw data for Locus 5

Loot 3 Locus 6

Box	Bag	Bag/Box	Classifications of fragments	Measurement	Age	Notes	Sex
2	1 of 6		cervical 1 vertebra		adult	fused bone	
			left ulna	25.5 cm	adult		
			skull fragment	49.93mm			
			rib shaft fragment	81.10mm			
			rib shaft fragment rib 2	54.20mm			
			rib shaft fragment	52.39mm			
			rib shaft fragment	51.19mm			
			rib shaft fragment	35.44mm			
			rib shaft fragment	51.83mm			
			rib shaft fragment	36.07mm			
			rib shaft fragment	30.88mm	subadult	very small	
			rib shaft fragment	28.77mm			
			vertebrae arch fragment	38.80mm			
			vertebrae fragment	18.39mm			
			vertebrae fragment	17.67mm			
			vertebrae arch fragment	41.09mm			
			tibia proximal epiphysis	44.99mm	potential subadult	it is small but also fragmented	
			distal epiphysis of femur	53.15mm			
			distal epiphysis of femur	47.62mm			
			right patella	39.39mm	adult		
			ulna proximal epiphysis	29.40mm	subadult	not fused	
			unidentifiable side metatarsal proximal end fragment	55.46mm			
			proximal hand phalange	41.57mm			
			unidentifiable metacarpal 1	32.79mm			
			unidentifiable metatarsal distal end fragment	22.93mm			
			unidentifiable metatarsal fragment	54.57mm			

Box	Bag	Bag/Box	Classifications of fragments	Measurement	Age	Notes	Sex
			unidentifiable side metatarsal 1 fragment	60.29mm			
			unidentifiable side metatarsal proximal end fragment	36.31mm			
			unidentifiable side metatarsal proximal end fragment	29.05mm			
			distal phalange fragment	18.28mm			
			distal hand phalange	26.73mm			
			proximal foot phalange	23.33mm			
			intermediate foot phalange	13.11mm			
			unidentifiable side metatarsal 1 fragment	23.46mm			
			proximal foot phalange	25.96mm			
			distal foot phalange	25.17mm			
			proximal foot phalange	25.04mm			
			proximal foot phalange	20.35mm			
			intermediate hand phalange	26.22mm			
			intermediate hand phalange	20.19mm			
			distal phalange	14.13mm	subadult	grooves on proximal epiphysis	
			right trapezoid	16.67mm			
			left cuneiform	23.26mm			
3	1 of 3	in tissue paper	upper maxilla fragment			RC1 and RP3 still in situ; loose tooth	
		found near a pot base (was rebagged)	skull fragment	60.30mm			
			skull fragment	37.04mm			
			skull fragment	38.31mm			
			skull fragment	25.80mm			
			skull fragment	36.31mm			
			right zygomatic bone	46.76mm			

Box	Bag	Bag/Box	Classifications of fragments	Measurement	Age	Notes	Sex
			right temporal bone	53.49mm		mastoid process fragmented; unable to determine sex	

Table D.6: Raw data for Locus 6

Loot 3 Locus 99

Box	Bag	Bag/Box	Classifications of fragments	Measurement	Age	Notes	Sex
1	2 of 14		left distal end humerus	46.07mm			
			right proximal ulna head	50.32mm			
			right metacarpal	42.64mm			
			intermediate hand phalange	24.99mm			
			proximal hand phalange	47.01mm			
			unidentified side proximal metatarsal base	45.16mm			
			left metacarpal	33.09mm			
			vertebrae	31.31mm			
			vertebrae	45.49mm			
			proximal hand phalange	34.86mm			
			intermediate hand phalange	29.16mm			
			phalange	25.25mm			
			right metatarsal	69.15nn			
			proximal hand phalange	38.98mm			
			right metatarsal 5	53.89mm			
			vertebrae spinous process	40.74mm			
			unidentified side metatarsal	37.09mm			
			unidentified side metacarpal	27.11mm			
			left rib	58.15mm		costal groove, tubercle	
			right femur head	72.02mm			
			left humerus head	48.21mm			
			left mandibular condyle process	26.67mm			
			vertebrae spinous process	26.87mm			
			thoracic vertebrae lamina & superior articular facet	38.12mm			
			unidentified side metatarsal 1	50.37mm			

Box	Bag	Bag/Box	Classifications of fragments	Measurement	Age	Notes	Sex
			proximal hand phalange	46.86mm			
			right metatarsal	46.06mm			
			proximal hand phalange	43.56mm			
			proximal hand phalange	35.65mm			
			intermediate hand phalange	23.63mm			
			proximal foot phalange	24.02mm			
			intermediate hand phalange	24.17mm			
			intermediate hand phalange	24.49mm			
			vertebrae spinous process	27.66mm			
			proximal hand phalange	28.86mm			
			right patella	47mm			
			right medial condyle; femur	58.95mm			
			occipital bone	67.14mm		occipital sulcus	
			left (?) parietal	74.44mm		meningeal lines	
			superior articular facet of thoracic vertebrae	26.27mm			
			mamillary process of lumbar vertebrae	34.20mm			
			transverse process; lamina; pedicle of thoracic vertebrae	28.32mm			
			femur head	41.15mm		hole straight through top of femur head	
			femur head	43.21mm		notch in head	
			unidentified side calcaneus	44.09mm			
			right radial shaft	60.53mm		oblique line and interosseous crest	
			right tibia proximal head	36.20mm		lateral condyle	
			manubrium	54.64mm			
			right rib	37.26mm			
			femur shaft	85.46mm			
			left humerus shaft	83.56mm		deltoid tuberosity;	
			vertebral spinous process and lamina fragment	19.07mm			

Box	Bag	Bag/Box	Classifications of fragments	Measurement	Age	Notes	Sex
			right radius shaft	64.11mm		radial tuberosity	
			long bone shaft fragment	80.62mm			
			right proximal end ulna head	35.08mm			
			right rib shaft	36.10mm			
			rib shaft	38.72mm			
			spinous process	24.73mm			
			intermediate hand phalange	25.55mm			
			proximal foot phalange	24.54mm			
			right metacarpal proximal end	30.47mm			
			proximal hand phalange	29.74mm			
			intermediate hand phalange	22.26mm			
			left metacarpal proximal end	43mm			
			proximal hand phalange	27.41mm			
			unidentifiable side metacarpal shaft	42.56mm			
			proximal hand phalange	31.14mm			
			femur head	35.28mm			
			vertebral lamina	35.90mm			
			phalange shaft	24.53mm			
			occipital bone	56.20mm		occipital sulcus	
			occipital bone	64.82mm		external occipital crest	
			left floating rib	32.72mm			
			left talus fragment	45.51mm			
			left lateral border	56.11mm			
			skull fragment	66.02mm			
			skull fragment	43.68mm			
			skull fragment	23.28mm			
			tibial shaft fragment	46.44mm		straight edge	
			half of a patella right (?)	36.97mm			
			skull fragment	51.02mm			

Box	Bag	Bag/Box	Classifications of fragments	Measurement	Age	Notes	Sex
			skull fragment	45.82mm			
			vertebrae body	32.61mm			
			foot phalange	23.68mm			
			left pisiform	15.80mm			
			left scaphoid	29.70mm			
			rib shaft	30.19mm			
			mandible fragment - tooth root	20.58mm			
			proximal foot phalange	22.29mm			
			vertebrae body	17.50mm			
			tibial shaft fragment	46.77mm		straight edge	
			unidentified side talus fragment	48.19mm			
			tibial proximal head	48.06mm			
			vertebrae fragment	21.70mm			
			orbital bone	23.76mm			
			unidentified side metatarsal head	15.85mm			
2	1 of 14		proximal hand phalange	47.29mm		lipping on sides	
			distal end of humerus	73.65mm			
			right floating rib	43.86mm			
			skull fragment	34.52mm		suture lines	
			skull fragment	60.20mm		suture lines	
			right patella	33.56mm			
			right patella	35.07mm			
			rib body	54.14mm			
			vertebral body	26.16mm			
			vertebral body	29.33mm			
			vertebral body	33.07mm			
			head & neck of rib	35.43mm			
			left metacarpal fragment	49.04mm			
			intermediate hand phalange	22.57mm			

Box	Bag	Bag/Box	Classifications of fragments	Measurement	Age	Notes	Sex
			proximal hand phalange	32,71mm			
			intermediate hand phalange	23.43mm			
			intermediate hand phalange	27.10mm			
			intermediate hand phalange	26.57mm			
			intermediate foot phalange	12.31mm			
			unidentified side metatarsal proximal end	28.01mm			
			left metatarsal head	29.94mm			
			left metatarsal head	18.10mm			
			proximal foot phalange	24.92mm			
			intermediate hand phalange	27.54mm			
			proximal foot phalange	23.86mm			
			intermediate hand phalange	23.19mm			
			intermediate hand phalange	22.62mm			
			intermediate hand phalange	22.05mm			
			distal hand phalange	20.66mm			
			right scapula	29.64mm		scapular spine	
			right temporal bone	60.78mm			
			skull fragment	40.59mm			
			skull fragment	40.14mm			
			skull fragment	31.62mm			
			radial head	17.36mm			
			patella fragment	24.50mm			
			temporal bone fragment	27.53mm			
			vertebral body	20.67mm			
			patella fragment	30.33mm			
			rib fragment	37.13mm			
			rib fragment	31.12mm			
			rib fragment	37.24mm			
			patella fragment	26.15mm			

Box	Bag	Bag/Box	Classifications of fragments	Measurement	Age	Notes	Sex
			rib fragment	22.65mm			
			unidentified side metacarpal distal end	19.64mm			
			intermediate hand phalange	16.49mm			
			phalange shaft	22.04mm			
			rib fragment	41.70mm			
			proximal foot phalange	27.72mm			
			intermediate hand phalange	29.88mm			
			intermediate hand phalange	21.71mm			
			rib fragment	26.68mm			
			intermediate hand phalange	19.10mm			
			intermediate foot phalange	14.62mm			
			proximal foot phalange	18.74mm			
			distal hand phalange	16.91mm			
			distal foot phalange	18.83mm			
			intermediate hand phalange	10.57mm			
			proximal hand phalange	20.95mm			
			intermediate hand phalange	21.02mm			
			vertebrae spinous process	23.95mm			
			intermediate hand phalange	14.59mm			
			vertebrae spinous process fragment	18.65mm			
			proximal foot phalange	15.17mm			
			proximal foot phalange	24.71mm			
			distal hand phalange	14.27mm			
			intermediate hand phalange	17.77mm			
			intermediate foot phalange	21.61mm			
			tibial shaft fragment	69.71mm			
			proximal foot phalange	24.86mm			
			rib fragment	41.37mm			
			intermediate hand phalange	30.39mm			

Box	Bag	Bag/Box	Classifications of fragments	Measurement	Age	Notes	Sex
			right tarsal fragment	44.44mm			
			pelvic border (?)	51.71mm			
			rib fragment	37.18mm			
			right calcaneus fragment	64.89mm			
			femur shaft	54.42mm			
			unidentified side metatarsal	39.72mm			
			rib fragment	45.84mm			
			rib fragment	42.46mm			
			humerus head (?)	30.13mm			
			skull fragment	59.87mm			
			skull fragment	38.76mm			
			skull fragment	30.43mm			
			skull fragment	29.62mm			
			skull fragment	30.76mm			
			skull fragment	35.09mm			
			skull fragment	25.11mm			
			skull fragment	22.31mm			
			vertebrae fragment	26mm			
			distal foot phalange	14.14mm			
			unidentified side metatarsal fragment	33.78mm			
			vertebrae fragment	28.37mm			
			humerus head (?)	17.36mm			
			hand phalange	25.67mm			
			left metatarsal fragment	41.29mm			
	1 of 12		right radial proximal end	47.22mm	subadult	approximately 7 years or younger; fovea not formed	
			femur head	51.42mm	adult		
			vertebrae body	54.23mm	adult		
			vertebrae body	32.93mm			
			intermediate hand phalange	46.04mm			

Box	Bag	Bag/Box	Classifications of fragments	Measurement	Age	Notes	Sex
			left metacarpal head	32.85mm			
			ulnar head	58.26mm	subadult		
			right patella	39.76mm	adult		
			tibia head proximal	34.51mm	subadult	grooved auricular surface	
			left patella	32.62mm	adult	muscle lines	
			proximal hand phalange	33.48mm			
			intermediate hand phalange	19.11mm			
			distal hand phalange	17.66mm			
			intermediate hand phalange	22.02mm			
			right metacarpal head	50.74mm			
			proximal hand phalange	31.59mm			
			distal foot phalange	22.99mm			
			distal hand phalange	17.37mm			
			intermediate hand phalange	22.98mm			
			intermediate hand phalange	23.31mm			
			unidentifiable side metatarsal 1 fragment	56.61mm			
			femur head	28.65mm	subadult	blunt projection- approx. 8 years or older	
			tibial head proximal end	36.57mm	subadult		
			rib fragment	50.22mm			
			rib fragment	50.55mm			
			rib fragment	39.92mm			
			rib fragment	36.74mm			
			rib fragment	43.48mm			
			rib fragment	53.92mm			
			distal hand phalange	15.88mm			
			distal hand phalange	15.12mm			
			right metacarpal 3 fragment	34.98mm			
			proximal foot phalange	27.48mm			
			proximal hand phalange	33.57mm			

Box	Bag	Bag/Box	Classifications of fragments	Measurement	Age	Notes	Sex
			proximal foot phalange	26.45mm			
			right metacarpal head	17.72mm			
			proximal hand phalange	12.49mm			
			rib fragment	28.69mm			
			rib fragment	38.44mm			
			rib fragment	38.13mm			
			rib fragment	29.80mm			
			femur head	17.64mm	subadult	blunt projection- approx. 3 years or older	
			proximal hand phalange	23.02mm			
			rib fragment	25.50mm			
			proximal hand phalange	27.29mm			
			phalange fragment	16.05mm			
			proximal hand phalange	20.30mm			
			proximal foot phalange	25.06mm			
			proximal hand phalange	17.85mm			
			skull fragment	39.62mm			
			skull fragment	31.77mm			
			skull fragment	29.78mm			
			skull fragment	34.01mm			
			skull fragment	27.54mm			
			skull fragment	24.61mm			
			skull fragment	24.17mm		suture lines	
			skull fragment	19.84mm	subadult	suture lines; not fused	
			skull fragment	25.92mm		muscle lines? On the border	
			vertebrae body	28.89mm	subadult	vascular grooves	
			vertebrae body	25.48mm	adult	defined border	
			vertebrae body	20.70mm	adult	defined border	
			vertebrae body	32.47mm	adult	defined border	
			vertebrae body	27.27mm	adult	defined border	

Box	Bag	Bag/Box	Classifications of fragments	Measurement	Age	Notes	Sex
			vertebrae body	28.79mm	adult	defined border	
			vertebrae body	28.91mm	adult	defined border	
			vertebrae body	18.32mm	adult	defined border	
			distal hand phalange	17.37mm			
			distal hand phalange	17.26mm			
			vertebral arch	30.87mm			
			cervical vertebrae	21.54mm	adult	transverse foramen; transverse process	
			vertebrae arch	27.58mm	possible subadult		
			vertebrae fragment	47.79mm			
			vertebrae fragment	30.12mm			
			vertebrae fragment	19.48mm			
			vertebrae fragment	18.40mm			
			head and neck of femur	63.62mm	possible subadult		
			vertebrae fragment	42.13mm	adult		
			vertebrae arch	35.17mm			
			femur head fragment	35.55mm			
			vertebrae fragment	27.66mm	subadult(?)		
			vertebrae fragment	17.65mm			
			vertebrae fragment	20.04mm			
			unidentifiable side metatarsal fragment	64.14mm			
			vertebrae body	25.25mm	subadult	vascular grooves	
			head of humerus or femur	29.81mm			
			right talus fragment	33.32mm			
			intermediate hand phalange	22.95mm			
			distal hand phalange	21.34mm			
			left metatarsal	75.39mm			
			right proximal end of metacarpal	30.79mm			
			skull fragment	23.41mm			

Box	Bag	Bag/Box	Classifications of fragments	Measurement	Age	Notes	Sex
			skull fragments in tissue paper			sutures visible only on 4 fragments	
	12 of 12	in box- 4	thoracic vertebrae	35.70mm	adult		
				30.27mm			
				29.58mm			
				28.96mm			
			vertebrae arch	41.25mm			
			vertebrae arch	38.25mm			
	2 of 12	bag within box 12 of 12	vertebrae body	41.30mm	adult		
			vertebrae body	29.58mm	subadult		
			intermediate hand phalange	29.84mm			
			vertebrae spinous process fragment	34.06mm			
			vertebrae body	28.36mm			
			vertebrae body fragment	31.07mm			
			left (?) ischium bone with auricular surface and ramus ridge	39.43mm	subadult	6months-1 year	
			proximal phalange	7.82mm	subadult- possibly child		
			intermediate hand phalange	23.67mm			
			left metacarpal fragment	35.44mm		head and piece of shaft	
			proximal foot phalange	24.48mm		lipping on sides of phalange - possible osteoarthritis	
			intermediate hand phalange	28.15mm		lipping on sides of phalange - possible osteoarthritis	
			distal hand phalange	17.24mm			
			intermediate hand phalange	32.58mm			
			left metatarsal	60.45mm			
			right metatarsal head	33.18mm			

Box	Bag	Bag/Box	Classifications of fragments	Measurement	Age	Notes	Sex
			unidentifiable side metatarsal head fragment	12.91mm			
			unidentifiable side metacarpal head	23.40mm			
			intermediate hand phalange	24.06mm			
			hand phalange head fragment	19.03mm			
			hand phalange head fragment	15.21mm			
			proximal foot phalange	19.42mm			
			rib fragment	30.20mm			
			rib fragment	35.19mm			
			left (?) rib fragment	55.70mm			
			rib fragment	33.54mm			
			distal first foot phalange	18.52mm			
			right patella	32.38mm			
			intermediate foot phalange	13.74mm			
			spinous process	23.60mm	possible adult		
			rib fragment	33.02mm			
			distal end of phalange	17.14mm			
			vertebrae fragment	29.18mm		lipping	
			skull fragment	22.58mm			
			skull fragment	36.55mm			
			left pisiform fragment	19.41mm			
			left scaphoid fragment	25.02mm			
			right hamate	24.93mm			
			unidentified side tarsal fragment	33.96mm			
			right tarsal fragment	38.25mm			
			left cuneiform	28.53mm			
			right cuneiform	28.40mm			
			right cuneiform	32.36mm			
			right metatarsal 4	67.02mm			

Box	Bag	Bag/Box	Classifications of fragments	Measurement	Age	Notes	Sex
			distal posterior femur	35.65mm	subadult- approx. 8-12 years old	defined borders	
	1 of 6		skull fragment	28.99mm			
			skull fragment	27.82mm			
			skull fragment	22.25mm			
			right patella	40.56mm			
			left (?) patella	36.70mm			
			rib fragment	36.06mm			
			vertebrae fragment	18.09mm	adult	defined border	
			vertebrae body fragment	24.39mm	adult		
			vertebrae body fragment	20.08mm	subadult	grooved surface	
			vertebrae body fragment	30.66mm	adult		
			vertebrae body fragment	24.86mm	subadult- approx. 6 year old	grooved surface	
			vertebrae fragment	24.24mm			
			vertebrae fragment	14.02mm			
			vertebrae fragment	23.29mm			
			vertebrae body fragment	14.86mm		defined border	
			vertebrae fragment	14.91mm			
			vertebrae fragment	16.52mm			
			vertebrae fragment	16.01mm			
			cervical vertebrae	45.76mm	adult?	defined border over the body of the vertebrae	
			intermediate hand phalange	21.58mm			
			intermediate hand phalange	19.22mm			
			intermediate hand phalange	15.68mm			
			distal hand phalange	17.68mm			
			proximal hand phalange	26.35mm			

Box	Bag	Bag/Box	Classifications of fragments	Measurement	Age	Notes	Sex
			intermediate hand phalange	15.30mm			
			proximal hand phalange	22.49mm			
			proximal hand phalange	24.46mm			
			proximal hand phalange	19.70mm			
			proximal hand phalange	22.72mm			
			proximal hand phalange	27.43mm			
			intermediate hand phalange	25.86mm		bone growth on the sides	
			distal foot phalange	12.73mm			
			proximal foot phalange	24.08mm			
			proximal foot phalange	20.02mm			
			unidentified side metacarpal head	18.66mm			
			intermediate hand phalange head	12.45mm			
			distal hand phalange	18.56mm			
			left metacarpal 4 proximal end fragment	27.69mm			
			right metatarsal head fragment	32.99mm			
			femur head fragment	34.13mm			
			proximal epiphysis of radius	17.50mm	subadult- approx. 10 years old	fovea present	
			base of proximal phalange	17.11mm	subadult - approx. 12-14 years old	sharp medial border; blunt lateral border	
			right scaphoid	23.11mm	possible subadult		
			possible subadult rib				
			potential subadult mandible fragment with tooth outline	19.82mm			
			possible skull zygomatic fragment	30.63mm			
			clavicle fragment				
			right trapezoid	15.06mm			
			distal end of femur	35.29mm	subadult		

Box	Bag	Bag/Box	Classifications of fragments	Measurement	Age	Notes	Sex
	12 of 14		unidentifiable side metacarpal	71.08mm			
			intermediate hand phalange	24.96mm		lipping on the side	
			unidentifiable side metacarpal 1	32.21mm			
			unidentifiable side metacarpal	48.10mm			
			intermediate foot phalange	12.33mm			
			intermediate hand phalange	26.07mm			
			distal end of humerus fragment	26.54mm			
			long bone shaft fragment	55.56mm			
			long bone shaft fragment	53.72mm			
			long bone shaft fragment	44.32mm			
			proximal hand phalange fragment	20.42mm			
	4 of 6		proximal epiphysis of radius	14.32mm	subadult	fovea present	
			distal epiphysis of long bone- possible radius	17.07mm	subadult	grooves present	
3	3 of 14	in bag	maxilla fragments				
		in tissue paper	skull fragments				
			left patella	43.56mm			
			femur head fragment	20.30mm	subadult		
			femur head fragment	21.24mm	subadult		
			femur distal end fragment	43.46mm			
			humeral head	39.27mm	adult		
			tibial proximal end	41.89mm	subadult		
			femur head fragment	36.62mm	subadult	one of the condyles	
			radial head fragment	17.31mm	subadult		
			vertebrae body fragment	24.32mm	subadult		
			right talus fragment	46.04mm	adult		

Box	Bag	Bag/Box	Classifications of fragments	Measurement	Age	Notes	Sex
			right talus fragment	40.43mm	adult?	grooved epiphysis end, very fragmented though- cant tell which long bone	
			unidentified side talus fragment	34.71mm	possible subadult?	very small	
			rib shaft fragment	37.45mm			
			rib shaft fragment	59.87mm			
			rib shaft fragment	38.80mm			
			rib shaft fragment	51.37mm			
			rib shaft fragment	40.97mm			
			rib shaft fragment	39.52mm			
			left navicular fragment	25.55mm	possible subadult?	small	
			left navicular fragment	40.35mm	adult		
			vertebrae body fragment	43.62mm	subadult		
			left cuneiform fragment	24.51mm	adult?		
			left metatarsal 4	40.24mm			
			right metacarpal 2	59.69mm			
			left metacarpal 2	45.36mm			
			left trapezoid	15.15mm			
			right metacarpal 4	29.11mm			
			right metacarpal 1	38.85mm			
			proximal hand phalange	37.65mm		lipping on sides	
			proximal hand phalange	23.40mm			
			proximal hand phalange	37.49mm		lipping on sides	
			intermediate hand phalange	21.26mm			
			intermediate hand phalange	29.43mm			
			distal 1 hand phalange	21.56mm			
			proximal foot phalange	21.70mm			
			proximal foot phalange	21.45mm			
			proximal hand phalange	28.91mm			

Box	Bag	Bag/Box	Classifications of fragments	Measurement	Age	Notes	Sex
			skull fragment	40.88mm		significant closure	
			skull fragment	45.56mm		significant closure	
			skull fragment	34.18mm		significant closure	
			skull fragment	19.54mm		significant closure	

Table D.7: Raw data for Locus 99